An asymptotic approximation of the maximum runup produced by a Tsunami wave train entering an inclined bay with parabolic cross section

N Postacioglu, M.S. Özeren, and Ebubekir Çelik

Technical University of Istanbul

(Dated: May 1, 2020)

Abstract

Investigation of the behavior of various types of Tsunami wave trains entering bays is of practical importance for coastal hazard assessments. The linear shallow water equations admit two types of solutions inside an inclined bay with parabolic cross section: Energy transmitting modes and decaying modes. In low frequency limit there is only one mode susceptible of transmitting energy to the inland tip of the bay. The decay rates of decaying modes are controlled by the boundary conditions at the sides of the bay. Therefore a complicated eigenvalue problem needs to be solved in order to compute these decay rates. To determine the amplitude of the energy transmitting mode one should solve an integral equation, involving not just the energy transmitting mode but also decaying modes, the scattered field into the open sea, the incident wave and the reflected wave in the open sea. However, in the long wave limit, all these complications can be avoided if one applies the Dirichlet boundary conditions at the open boundary. That is to take the displacement of the free surface at the open boundary being equal to the twice of the disturbance associated with the incident wave in the open sea, just like a wall boundary condition. The runup produced by the solution obtained from this Dirichlet boundary condition, can be easily calculated using a series of images. In this model no energy is allowed to escape from the bay therefore the error arising from the simplification of the boundary conditions at the open boundary grows with time. Nevertheless the maximum runup occurs before this error becomes significant. If the characteristic wavelength of the incident wave train is equal to 5 times the width of the bay then this simple solution overestimates the first maximum of the runup only b %15 compared to the "exact" solution derived from the integral equation. This overestimation is partly due to the fact that Dirichlet boundary conditions violates the continuity of depth integrated velocities. The solution associated with Dirichlet boundary condition is perturbed in order to match fluxes inside and outside of the bay. This perturbation does not use the decaying modes inside the bay. The height of the first maximum of the runup coming from the perturbation theory is in excellent agreement with that obtained using the integral equation. This perturbation theory can also be applied to narrow bays with arbitrary cross section as long as their depth does not not change in the longitudinal direction.

I. INTRODUCTION

Waves grow as they approach the shoreline due to the decreasing water depth. This is valid for all shoaling bathymetries and is even more pronounced in converging bays. The behavior of waves in the vicinity of shoreline has been an active research topic for long time ([1–3]). Most of these analytical and numerical models consider a wave train of various shapes progressing first over a flat ocean and then making a passage over a sloping bathymetry leading to the beach. Let us look at the one-dimensional version of the problem which has important practical applications in the context of Tsunamis and storm surges . An obvious difficulty for both analytical and numerical studies is the nature of the open boundary condition offshore. The reason this is difficult is that, after a certain time the waves will start getting reflected from various features of bathymetry and the shoreline itself. Since this reflecting wave field is unknown at the offshore boundary, it is not clear how to pose the boundary value problem. To overcome this difficulty, authors [4] turned this into an initial value problem where they imposed the value of the free surface at the offshore boundary point in a particular way in which it remained equal to the twice of the vertical displacement of the free surface generated by the incident wave arriving from the open sea. They also assumed an initially flat free surface between the offshore boundary and the shoreline. They then calculated the nonlinear wave evolution subject to this boundary condition at all times. In this, they observe a strong resonant regime. Indeed such resonance has been confirmed in the later studies ([5, 6]) in the presence of large slope discontinuity. In a past paper [7] we criticized [4] because their model trapped perfectly the energy of the waves over the slope because of their boundary condition. In their model, if the incoming monochromatic wave has the same frequency as the resonant frequency, the amplitude of the standing waves over the slope will increase with time in an unbounded fashion. What we overlooked in our criticism, however, was that, if there is a large depth discontinuity at the offshore boundary point then their boundary condition will lead to an accurate estimation of the wave over the uneven bathimetry for a limited time scale. Tsunamis being short-lived phenomena, this limited timescale can be sufficient to compute their maximum runup. To see the validity of their boundary condition one may consider a very simple geometry where an ocean of uniform depth H_0 is connected to a shallow shelf of depth H_1 with $H_0 \gg H_1$.

Let x_0 be the length of the shallow shelf. If the incident wave has the form

$$I_0\theta\left(\sqrt{gH_0}t+(x-x_0)\right)\exp\left(i\omega\left(t+\frac{x-x_0}{\sqrt{gH_0}}\right)\right) \tag{1}$$

where θ is the step function ($\theta(x)=1$ if $x>0$ else it is zero), g is the acceleration due to gravity. It is easy to see that the major part (almost all) of the energy of the incident wave will be reflected back at $x=x_0$ which is the toe of the shallow shelf. This is due to the very large depth contrast and the toe acting almost like a solid vertical wall. Note here that the transmitted power of a linear shallow water (LSW) wave at any given point is equal to $Hu\rho g\eta$ where H,u,ρ,g and η are water depth, fluid velocity, water density, acceleration of gravity and the free surface vertical displacement respectively. Hence, at the toe, the depth-averaged fluid velocity being almost zero, only a very small part of the power is transmitted onto the shelf. This means that the incident and reflected waves will be superimposed at $x=x_0^+$, leading to an oscillation with amplitude equal to $2I_0$ there. This oscillation will trigger a progressive wave towards the shore with amplitude $2I_0$. This wave will be reflected from the shoreline and will arrive back to the toe. There, a tiny part of it will be transmitted onto the open ocean and the amplitude of this will be

$$\frac{4I_0\sqrt{H_1}}{\sqrt{H_0}+\sqrt{H_1}}\ll 2I_0\,. \tag{2}$$

Therefore the perturbation of the offshore boundary condition will be negligible. The process will continue, setting up a standing wave regime over the shelf, with an amplitude increasing with time (until the steady regime is reached due to the wave radiation into the open sea) because the incident wave will keep arriving. Although only a tiny percentage of this standing wave will create a transmission towards offshore, it too will increase with time and may become of the same order of $2I_0$.

For a monochromatic incident wave with a frequency matching the first resonant frequency of the shallow shelf ($\omega_1=\sqrt{gH_1}\pi/(2x_0)$), it can easily be shown that the *steady* solution is given as

$$\eta(t,x)=\begin{cases}2I_0\sqrt{H_0/H_1}\cos(\frac{\pi}{2x_0}x)\exp(i\omega_1 t) & \text{for}\quad 0<x<x_0\\ 2I_0\sin\left(\frac{\pi}{2x_0}\sqrt{\frac{H_1}{H_0}}(x-x_0)\right)\exp(i\omega_1 t) & \text{for}\quad x>x_0.\end{cases} \tag{3}$$

In the second line of the above formula, the sine term corresponds to the superposition of the incident wave and the reflected wave, thus indicating radiation towards the open ocean. This

particular steady solution maintains $\eta = 0$ at the toe during the steady regime. This shows that, when the steady regime is reached, the boundary condition $\eta = 2I_0$ at the toe becomes irrelevant. To calculate the time necessary to reach the steady state, note first that the steady solution above does not satisfy the initial condition, $\eta(t = 0, x) = 0$, over the shallow shelf. Therefore the temporally decaying solutions of the homogeneous wave equation (not driven by the incident wave) need to be added to it. The decay time of these homogeneous solutions is the time necessary to reach the steady regime. Any wave corresponding to the homogeneous solution, travelling on the shallow shelf, when reflected by the toe of the shelf, gets its amplitude multiplied by $1 - 2\sqrt{H_1/H_0}$ for $H_1 \ll H_0$. The polarity is reversed each time such reflection occurs simply because the direction of propagation is from shallow to the deep. Such consecutive weak damping at the toe will erode the wave exponentially, leading to a wave proportional to $\exp\left(t \ln(1 - 2\sqrt{\frac{H_1}{H_0}}\,)/(2x_0/\sqrt{gH_1})\right)$ which approximately simplifies to $\exp(-t\ 2\sqrt{\frac{H_1}{H_0}}/(2x_0/\sqrt{gH_1}))$. Here $(2x_0/\sqrt{gH_1})$ is two-ways travel time of the wave over the shallow shelf.

Now let us elaborate on the the spatial and oscillatory behavior of these homogeneous solutions. These decaying solutions satisfy usual boundary conditions at the toe (continuity of the free surface and that of the depth integrated velocity). These homogeneous solutions transmit energy in the offshore direction. All these conditions can be satisfied at certain complex frequencies given by

$$\omega_n = \frac{\sqrt{gH_1}}{x_0}\left(\frac{\pi}{2} + n\pi + i\tanh^{-1}\left(\sqrt{H_1/H_0}\right)\right),\ n = 0, 1, 2... \tag{4}$$

where $\tanh^{-1}\sqrt{H_1/H_0}$ can be approximated by $\sqrt{H_1/H_0}$. The explicit form of these solutions is

$$\eta(t, x) = \begin{cases} \cos(\frac{\omega_n}{\sqrt{gH_1}}x)\exp(i\omega_n t) & \text{for} \quad 0 < x < x_0 \\ \cos(\frac{\omega_n}{\sqrt{gH_1}}x_0)\exp\left(i\omega_n\left(t - \frac{x-x_0}{\sqrt{gH_0}}\right)\right) & \text{for} \quad x > 0. \end{cases} \tag{5}$$

In a more complex geometry it is not possible to give an explicit expression for the complex frequencies of the homogeneous solutions. According to the linear theory Fourier transform of the runup is the Fourier transform of the incident wave at a given point multiplied by the response function. The frequencies of the homogeneous solutions are the poles of the response function in the complex plane. The response function for various geometries is given in [1, 6, 7].

Our discussion so far involved neither a bay nor a sloping bathymetry. The reason we investigated a simple step bathymetry so far is that it has a lot of relevance for non-reflecting bays where, once a wave enters it, the energy is transmitted all the way to the inland tip and reflects only from there. In [8] it was shown that only inclined bays of parabolic cross-section satisfy this condition. To start our discussion, consider an inclined bay of length x_0 with a parabolic cross-section which connects to a flat-bottomed open sea of depth H_0. Again, let us consider an incident wave , with a wavelength much larger than the width of the mouth of the bay ($2Y_0$). Unlike the one-dimensional case discussed above, there is no large depth discontinuity at $x = x_0$ but despite this, in this case too the incident wave will almost totally be reflected back at $x = x_0$. This is because the only horizontal length scale in the open ocean is the wavelength, λ. If the fluid velocity in the x direction, u, is averaged, in the y axis (perpendicular to the wave propagation direction) along a distance comparable to the wavelength, it will be almost zero at $x = x_0^+$, meaning an almost total reflection. Also, like in the one-dimensional case, the free surface disturbance at the mouth will be twice that of the incident wave. Thus, we have

$$\eta(t, x_0^-) = 2\eta^{\text{inc}}_{\text{open}}(t, x_0^+)\,. \tag{6}$$

This condition (hereafter we will refer to this as "Dirichlet" boundary condition) tends to slightly overestimate the runup because the *real* free surface disturbance is less than this at $x = x_0^-$ because of the partial penetration of the wave into the bay. The disturbance, $2\eta^{\text{open}}_{\text{inc}}\eta(t, x_0^+)$, will induce a progressive wave within the bay which will eventually be reflected from the inland tip. This reflected wave will arrive back to the mouth and there, it will reflect back towards the inland tip and its polarity gets reversed. To understand why the reflection is almost total, we need to investigate the free surface disturbance in the open sea produced by a hypothetical discharge from the bay starting at $t = 0$ and continuing at constant rate thereafter. The resulting free surface disturbance at the open sea will go quickly to zero for $t \gg Y_0/\sqrt{gH_0}$. This decay will be shown with help of Green's function associated with wave equation in 2D, $[\partial_{tt} - gH_0(\partial_{xx} + \partial_{yy})]\,\eta = 0$. The waves with wavelengths much larger than the width of the bay are almost constant at time scale $t_0 = Y_0/\sqrt{gH_0}$. Therefore the disturbance caused by the wave transmitted from the bay into the open sea is negligible unless the amplitude of the waves inside the bay are much larger than that of the incident wave in the open sea. Again, the time necessary for the growth of the standing waves inside

the bay is much larger than $2\tau_0$, τ_0 being the travel time of the wave along the length of the bay. In the following section, we will obtain the linear runup response of inclined bays of parabolic cross sections by averaging disturbance of the free surface across the lateral extent of the bay. The boundary condition at the bay mouth will be taken as equal to the twice the incident wave. In the section after this, we will consider the true boundary conditions where the continuities of *both* η and depth-integrated fluid velocities in the x direction are satisfied. To do this we have to take the scattered wave field in the open sea side and this scattered field may strongly depend also on the y coordinate. Therefore to ensure smooth transition of the waves in and out of the bay, we have to consider the fully two dimensional problem, at least in the vicinity of the mouth in both sides. Actually, there are studies([9, 10]) where the laterally averaged formulation is improved via the means of perturbative approaches. If the bay is narrow enough given an incident wavelength, there is only one mode that susceptible of transmitting energy within the bay. To understand that this is generally the case (irrespective of whether the bay having a parabolic cross-section), it is enough to look at the case of an infinitely long channel of rectangular cross section of width $2Y_0$. The dispersion relation of the waves that are symmetrical with respect to mid line is then

$$\omega^2 = gH_0(k_n^2 + (\pi n/Y_0)^2) \tag{7}$$

where k_n becomes purely complex when $n = 1, 2, \ldots$ These modes have strong y dependence even in the low frequency limit, therefore not suitable for a perturbative approach in the y direction. Because of the boundary conditions at the sides of the bay, two dimensional solutions of LSW leads to an eigenvalue problem. This eigenvalue problem is trivial if only the bay has uniform depth in y direction (see [7]).

In the last section, in order to estimate how much the *real* water level at the mouth of the bay is less than twice of the incident wave we perturb the Dirichlet boundary condition at the mouth using a dimensionless expansion parameter which is the ratio between the mouth width and the wavelength of the incident wave. We will demonstrate that such a perturbative approach will be useful to make an accurate estimation of the runup using a one dimensional propagation within the bay, thus avoiding complicated eigenvalue problems.

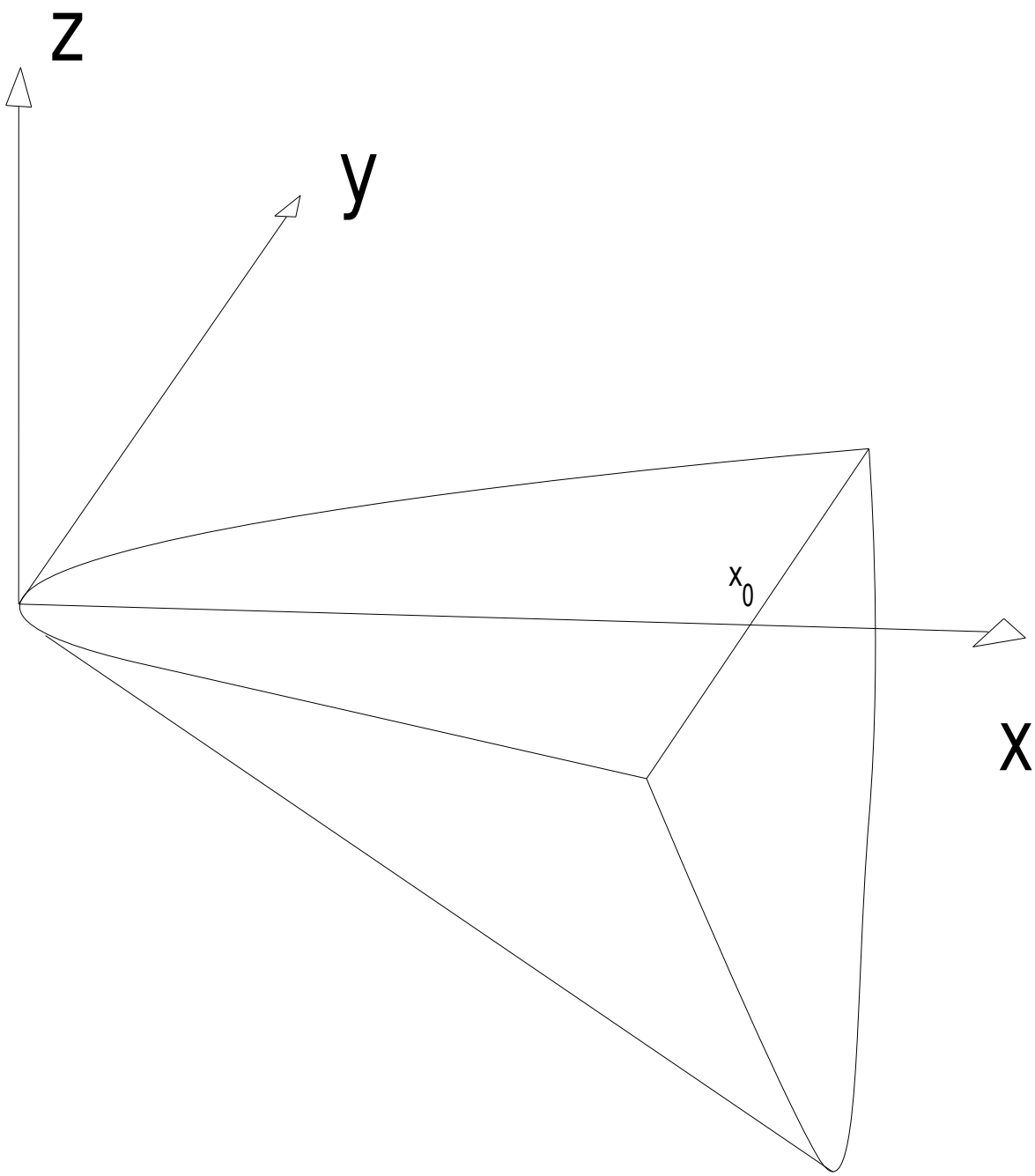

FIG. 1. The inclined bay opening to a semi infinite sea of uniform depth $H_0 = \alpha x_0$ where α is the slope of the inclined bay with parabolic cross section and x_0 is its length. The half width of the bay at its mouth is Y_0. The bottom of the bay is given by $z = -\alpha x + y^2/y_0$ with $H_0 = Y_0^2/y_0$.

II. DIRICHLET CONDITION AT THE MOUTH OF THE BAY

Let us consider an inclined bay with a parabolic cross section whose bottom coordinate is given by

$$z = -\alpha x + y^2/y_0 \tag{8}$$

where $z = 0$ is the undisturbed free surface. The half width of the bay at its entrance is then $Y_0 = \sqrt{\alpha y_0 x_0}$. The relation between the uniform depth H_0 of the open sea and the length of the bay is $H_0 = \alpha x_0$ (see Figure 1).

Let us consider a progressive wave with an intermediate wavelength advancing in converging bay of arbitrary shape. By intermediate wavelength it is meant a length scale much shorter than the bay length but still much larger than the bay width. For such wave the shape of the cross section of the bay does not vary much within one wavelength so that the transmitted power is preserved. The transmitted power is

$$S_0(x) g \rho \bar{\eta}(t,x) \bar{u}(t,x) \tag{9}$$

with $\bar{u}$ proportional to $\bar{\eta}/\sqrt{\bar{H}(x)}$ for a progressive wave (see [11] page 117). Here $S_0(x)$ is the undisturbed area of the cross section of the bay. Bars over the symbols denote the averaged values along the width of the bay. Due to the conservation of energy, the approximate form of the progressive wave inside a smooth bay of arbitrary shape is (see [12])

$$\bar{\eta}(t,x) \approx \int d\omega \frac{2\tilde{I}_0(\omega) \exp\left(i(\omega t + \int_{x_0}^{x} k(\omega, x')dx')\right)}{\sqrt{S_0(x)/S_0(x_0)}\left(\bar{H}(x)/\bar{H}(x_0)\right)^{-1/4}} \tag{10}$$

where $k(\omega, x)$ is $\omega/\sqrt{g\bar{H}(x)}$, and $\tilde{I}_0(\omega)$ is Fourier transform with respect to time of the incident wave train at $x = x_0^+$. For an inclined bay with parabolic cross section, S_0 is proportional to $x^{3/2}$ and $\bar{H}$ to x. Taking these relations into account (10) is reduced to

$$\bar{\eta}(t,x) \approx \int d\omega \frac{2\tilde{I}_0(\omega) \exp\left(i(\omega t + \int_{x_0}^{x} k(\omega, x')dx')\right)}{\sqrt{x/x_0}}\,. \tag{11}$$

In [8] it was shown that the solution above is an exact solution of LSW averaged over the width of the bay and it is valid up to the inland tip of the bay. Carrying out the integration with respect to x' and ω

$$\bar{\eta}(t,x) = 2\sqrt{\frac{x_0}{x}}\eta_{\text{inc}}^{\text{open}}\left(t - \sqrt{\frac{6}{\alpha g}}(\sqrt{x_0} - \sqrt{x}), x_0^+\right) \tag{12}$$

is obtained. These are called non-reflecting because the phase of a wave inside it is simply function of $t - \sqrt{6x/(\alpha g)}$. They, therefore, do not reflect until they arrive the inland tip of the bay. The reflected wave by the inland tip of the bay has opposite polarity to ensure that the power transmitted to the tip is zero. When the incoming and the reflected waves of opposite signs are added in the vicinity of the inland tip (x being infinitesimally small), the difference between their phases become proportional to $\sqrt{x}$ at a given instant t. At this limit, the water level becomes proportional to the zeroth power of x. This leads to a transmitted power of order of x. It was already mentioned that the wave that is travelling in the offshore direction when reflected by the mouth of the bay its polarity is reversed because these waves do no affect the water level at $x = x_0$. After two reflections the original polarity is recovered. A wave that progresses toward the mouth of the bay has undergone an odd number of reflections while a wave approaching the inland tip of the bay has been exposed to an even number of reflections (0,2,..). Summing all these reflections the profile of the wave can be found as

$$\bar{\eta}(t,x) = \sum_{k=0}^{\infty} 2\sqrt{\frac{x_0}{x}} \Bigg[\eta_{\text{open}}^{\text{inc}} \left(t + \tau_0 \sqrt{x/x_0} - (2k+1)\tau_0, x_0^+ \right) - \eta_{\text{open}}^{\text{inc}} \left(t - \tau_0 \sqrt{x/x_0} - (2k+1)\tau_0, x_0^+ \right) \Bigg] \tag{13}$$

where τ_0 is one way travel time along the bay ($\sqrt{6x_0/(\alpha g)}$). The resulting runup $r(t) = \eta(t, x = 0)$ according to [8] can be obtained using Hôspital rule. It is

$$r(t) = \sum_{k=0}^{\infty} 4\tau_0 \left[\frac{\partial}{\partial t} \eta_{\text{open}}^{\text{inc}} \left(t - (2k+1)\tau_0, x_0^+ \right) \right]. \tag{14}$$

Note that runup is proportional to the length of the bay because $\tau_0 = \sqrt{6x_0/(\alpha g)}$ is equal to $x_0/\sqrt{6H_0 g}$. For the case of the infinitely wide sloping beach of length x_0 connected to a sea of unfirom depth the runup is proportional to $\sqrt{x_0}$ if the wavelengths of incident wave are much smaller than x_0 (see [13]). Thus converging bays generate larger runup than those of the infinite sloping beaches.

According to Dirichlet condition the runup is a periodical function of time even though the incident wave train is not. In the next section we will show that when the series in (14) is truncated to its few terms it produces more realistic runups because of the radiation damping. An incident N-wave in the open sea may have slopes of the same sign in its front

and tail. If the distance between the regions of positive slopes is about $2\tau_0\sqrt{gH_0}$, then wave from these regions may interfere constructively to generate a larger runup.

If the the period of the incident wave in the open sea is much larger than the travel time (τ_0) of the waves along the bay then the summation in (14) can be seen as Riemann sum with integration step $2\tau_0$, and the runup will be approximated by

$$r(t) \approx 2\int_{-\infty}^{t} dt\, \frac{\partial}{\partial t}\eta_{\text{open}}^{\text{inc}} = 2\eta_{\text{open}}^{\text{inc}}\left(\sqrt{gH_0}\; t\right). \tag{15}$$

This was an expected result because with such long waves the displacement of the free surface at the tip and at the mouth of the bay must be equal. Note that this result is independent of any geometric characteristic (except the length) of the bay, reflecting the physical phenomenon of water slowly invading everywhere simultaneously, in a way reminiscent of the principle of communicating vessels.

To show the difference of behaviour of waves in reflecting and non-reflecting bays two infinitely long inclined bays are considered, one with parabolic cross section (non-reflecting) and the other with rectangular cross section and constant width. The slope of rectangular bay is $2\alpha/3$ so that both bays have the same averaged depth for a given x. In the non-reflecting bay, the wave train reflected by the inland tip is related to the initial incident wave trough the relation,

$$\bar{\eta}_{\text{ref}}(t,x) = -\sqrt{\frac{\tau^{-1}(t-\tau(x))}{x}}\eta_{\text{inc}}\left(t=0, x+\tau^{-1}\left(t-\tau(x)\right)\right)\theta(t-\tau(x)) \tag{16}$$

where function τ is $\sqrt{6x/(g\alpha)}$. Step function θ in the above equation is due to the fact that reflection starts at $t=0$. In the case of inclined rectangular bay, defining σ as $\sqrt{6x/(g\alpha)}$ a general solution of LSW averaged over the width of the bay becomes

$$\bar{\eta}(t,x) = \int_0^{\infty} d\omega\, J_0(\omega\sigma)\left[a(\omega)\cos(\omega t) + b(\omega)\sin(\omega t)/\omega\right] \tag{17}$$

according to [14]. Here J_0 is Bessel function of the zeroth order. Coefficients $a(\omega)$ and $b(\omega)$ can be obtained proceeding to Hankel transform of $\bar{\eta}(t=0,\sigma)$ and $\partial_t\bar{\eta}(t,\sigma)|_{t=0}$ respectively ($a(\omega) = \int_0^{\infty} d\sigma\sigma J_0(\omega\sigma)\bar{\eta}(t=0,\sigma)$). The wave given by (17) can emulate a wave which initially progresses toward the the coast if $\partial_t\bar{\eta}(t=0,x)|_{t=0}$ is equal to $\sqrt{gH(x)}\partial_x\bar{\eta}(t=0,x)$ according to [2] page 84 (assuming the breadth of the wave train is much less than the distance to the inland extremity of the inclined bay). The snapshots of the wave generated by equations 16 and 17 are displayed in Figure 2. Although these two examples share

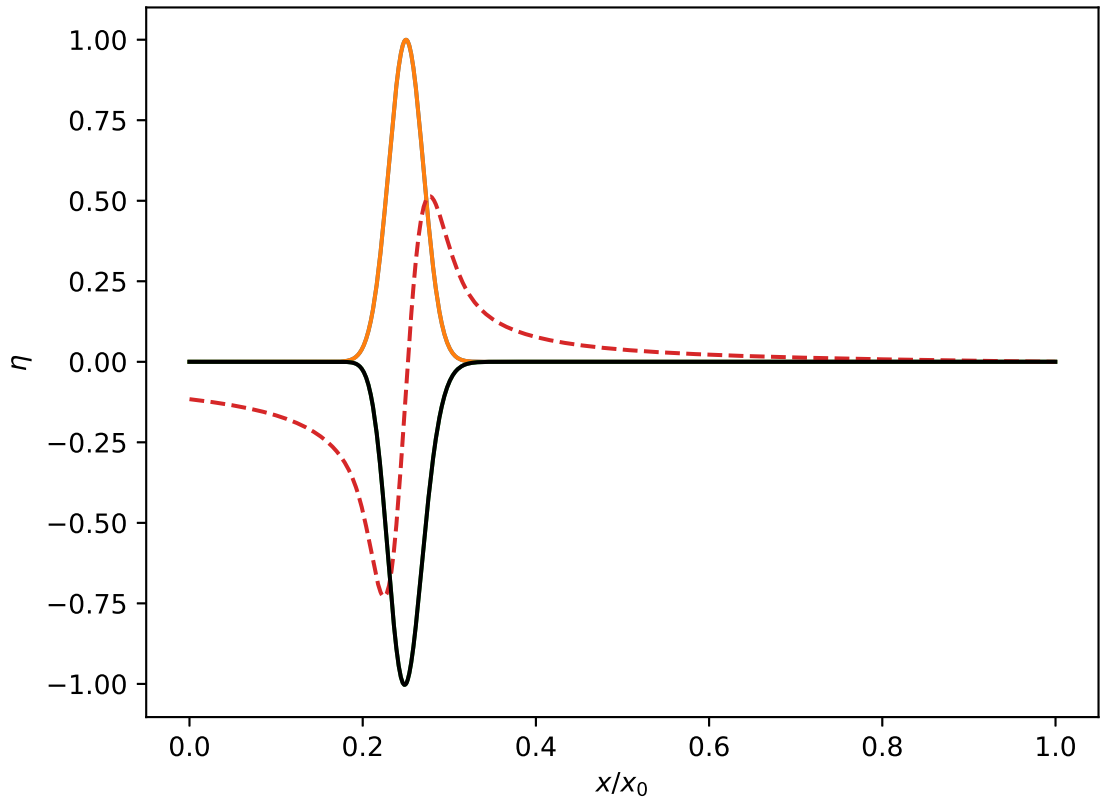

FIG. 2. The positive continuous curve is the initial profile of the incident wave given by $\exp\left[-\frac{1}{2}\left(\frac{x-x_1}{a}\right)^2\right]$ .The incident wave is progressing in an inclined bay with parabolic cross-section. The bottom of the bay is $z = -\alpha x + y^2/y_0$. The depression is the wave profile at instant $t = 2\int_0^{x_1} \frac{dx}{\sqrt{2g\alpha x/3}}$(the denominator in the integrand is the wave speed). The broken curve is the wave profile at instant t for the same incident wave progressing over a sloping bay with rectangular cross section whose slope is $\frac{2}{3}\alpha$. In both geometries the averaged depths for a given x are equal. The values of parameters are $x_1 = x_0/4, a = 0.02x_0$ (x_0 is an arbitrary length scale). Note that for the case of sloping bay with rectangular cross section the incident wave starts to be reflected before reaching $x = 0$.

the same initial conditions reflected wave in the case of reflecting bay reaches higher x coordinates than that of the non-reflecting bay because in the first case the wave starts to be reflected before reaching the inland tip of the bay. To understand the mechanism of continuous reflection in reflecting bays one can solve LSW using the transfer matrix method

(see [15]) where converging bays will be divided into piecewise channels of uniform cross section. In each piece the power transmitted by the offshore travelling wave will be different indicating reflections by the boundaries between the channels.

III. EXACT BOUNDARY CONDITIONS AT THE ENTRANCE OF THE BAY

In this section we will match η and $H(x,y)\partial_x\eta$ across the mouth of the bay. For this purpose two dimensional solutions of LSW must be found inside the bay. It was already mentioned that the solutions that depend strongly on y coordinates are confined to the vicinity of the mouth of the bay where the relative depth variation in x direction is small. Therefore the bay will be approximated by a channel of uniform cross section (basically a non-inclining channel of parabolic cross section) in this region.Two dimensional LSW equation is

$$\frac{\partial^2}{\partial t^2}\eta - g\left[\frac{\partial}{\partial x}\left(H\frac{\partial}{\partial x}\eta\right) + \frac{\partial}{\partial y}\left(H\frac{\partial}{\partial y}\eta\right)\right] = 0 \tag{18}$$

where H is $H_0(1-(y/Y_0)^2)$ in the vicinity of the mouth. For depth independent of x the solution of LSW is in the form

$$\eta_\omega = \exp\left(\kappa(\omega)x\right) f_\kappa\left(y\right) \exp\left(i\omega t\right) \tag{19}$$

where $\kappa(\omega)$ multiplied by i is the wavenumber within the parabolic channel. Defining non dimensional y' as y/Y_0, function f_κ must satisfy the the ordinary differential equation

$$-\frac{\omega^2 Y_0^2}{g\alpha x_0} f_\kappa(y') - \kappa^2 Y_0^2(1-y'^2) f_\kappa(y') - \frac{d}{dy'}\left\{(1-y'^2)\frac{d}{dy'}f_\kappa(y')\right\} = 0 \tag{20}$$

This ordinary differential equation has two singular points $y' = \pm 1$. Given ω (which we will take to be equal to the frequency of the incident wave), if parameter κ takes some discrete values, $\kappa_0(\omega), \kappa_1(\omega), ..$ then the solution will become regular at both singular points (our aim is to determine those particular κ values). In that case depth integrated non dimensional fluid velocity in y *direction*

$$(1-y'^2)\frac{d}{dy'}f(y')$$

will be zero at the sides of the channel ($y' \to \pm 1$). The situation is very similar to the case of rectangular channel where the n in (7) needed to be an integer in order to satisfy the no flux condition.

Equation(20) in terms of the wave vector of the incident wave($\omega = \sqrt{g\alpha x_0}\, k_{\text{inc}}^{\text{open}}$) becomes

$$\kappa^2 Y_0^2 (1-y'^2) f_\kappa(y') = -(k_{\text{inc}}^{\text{open}} Y_0)^2 f_\kappa(y') - \frac{d}{dy'}\left\{(1-y'^2)\frac{d}{dy'} f_\kappa(y')\right\} . \tag{21}$$

Only solutions that are even functions of y' will be taken into account because of the symmetry of the incident wave. Note that the eigenfunctions of the differential operator, $\frac{d}{dy'}\left\{(1-y'^2)\frac{d}{dy'}\right\}$, in the equation above, are Legendre polynomials

$$P_l(y')$$

with eigenvalues

$$-l(l+1) \quad \text{with } l = 0, 1, 2, \ldots .$$

We may write

$$f_\kappa(y') = \sum_{l=0}^{\infty} A_{2l}^{(\kappa)} \sqrt{2l+0.5} P_{2l}(y') . \tag{22}$$

Inserting the series above into (21) and using relations

$$\begin{cases} y' P_l(y') = \frac{1}{2l+1}\left((l+1)P_{l+1}(y') - l P_{l-1}(y')\right) \text{and } y' P_0(y') = P_1(y') \\ \frac{d}{dy'}\left\{(1-y'^2)\frac{d}{dy'}\right\} P_l(y') = -l(l+1) P_l(y') \end{cases} \tag{23}$$

the term, y'^2, and the derivatives of P_{2l} can be eliminated from the series. The left hand side of (21) is then reduced to a series of Legendre polynomials with constant coefficient involving $A_{2l}^{(\kappa)}$'s. Setting these coefficients to zero a recurrence relation between $A_{l-2}^{(\kappa)}$, $A_l^{(\kappa)}, A_{l+2}^{(\kappa)}$ is found. For the paticular case of $l = 0$, $A_2^{(\kappa)}$ is proportional to $A_0^{(\kappa)}$ with

$$A_2^{(\kappa)} / A_0^{(\kappa)} = -\frac{1}{2}\left[(k_{\text{inc}}^{\text{open}} Y_0)^2 + (\kappa Y_0)^2\right] .$$

For some discrete values of the eigenvalue, $(\kappa Y_0)^2$, coefficients $A_{2l}^{(\kappa)}$ obtained from the recurrence relation tend to zero for $l \to \infty$. The value of $A_0^{(\kappa)}$ is arbitrary. In appendix A an alternative method that is easier to implement in Python using linear algebra package is presented. Eigenvalues ($(\kappa Y_0)^2$) computed by the linear algebra package will be referred as 'exact' eigenvalues as they are more accurate than various approximations that will be made later. Ordinary differential equation given by (21) is similar to the differential equation for angular prolate spheroidal wave function (see equation 21.6.1 in[16]). In the context of the angular spheroidal differential equation the term denoted in (21) as ($k_{\text{inc}}^{\text{open}} Y_0$) is the quantity to be determined. This quantity is called in that context separation constant. Our

aim in solving LSW was to determine $(\kappa Y_0)^2$ as a function of the frequency of the incident wave. Because of this discrepancy the libraries for spheroidal functions were not used.

In Figure 3 the inverse of the relation between κ and ω is displayed (see Appendix A for the relation). In that figure one can observe that that given a non dimensional frequency $(\omega Y_0/\sqrt{g_0 H_0})$ less then $\sqrt{6}$ there is only one mode with negative $(\kappa Y_0)^2$ (continuous curve in Figure 3). Negative $(\kappa Y_0)^2$ corresponds to a real wave vector inside the bay. Our hypothesis was that the modes depending strongly on y coordinate are confined to the vicinity of the mouth of the bay. If there are two modes with real wave vector then the hypothesis will be violated as the second mode is roughly proportional to $P_2(y')$. Our analysis will be valid for $\omega Y_0/\sqrt{g_0 H_0} < \sqrt{6}$. The reason why the non dimensional cutoff frequency is exactly $\sqrt{6}$ will be clarified latter. Purely complex wave vector ($(\kappa Y_0)^2 > 0$) can not transmit power because u ad η will be off phase by $\pi/2$.

In an infinite rectangular channel of similar averaged depth $(2H_0/3)$, there will be only one energy transmitting mode if $\omega Y_0/\sqrt{gH_0}$ is less than $2.56 \approx \sqrt{2/3}\,\pi$. Note that the eigenvalues of the differential operator at the right hand side of (21) acting on even functions are

$$-(k_{\rm inc}^{\rm open} Y_0)^2 + 2l(2l+1) \quad \text{with} \quad l = 0, 1, 2, .. \tag{24}$$

For non dimensional frequency $(k_{\rm inc}^{\rm open} Y_0) < \sqrt{6}$, only the first eigenvalue (associated with $l = 0$) will be negative. When the differential operator at the right hand side of (21) is multiplied from left by the inverse of the positive operator, $(1 - y'^2) : f \to (1 - y'^2) f$, the number of negative eigenvalues does not change.

The eigenvalues, $(\kappa Y_0)^2$, will be numbered in ascending order:

$$(\kappa_0 Y_0)^2 < 0 < (\kappa_1 Y_0)^2 < (\kappa_2 Y_0)^2 < ... \tag{25}$$

Only mode 0 is then capable of transmitting energy. The dispersive nature of the relation between ω and $|\kappa_0 Y_0|$ becomes apparent for $|\kappa_0 Y_0| > 2$ where clearly

$$\frac{d^2}{dk^2}\omega < 0$$

with $k = i|\kappa_0|$. According to Figure 3 the approximation made by [10] for the dispersion relation is far better than that obtained from laterally averaging depth ($\omega = \sqrt{g\bar{H}}k$). However the dispersion relation in [10] slightly overestimates the frequencies(compare circles

with continuous curve in Figure 3). This *small* overestimation can be explained on the basis variational formulation of the eigenvalue problem.

In the above calculation, our aim was to calculate different κ values given ω, the frequency of the incident wave. Alternatively, we can calculate ω, given κ. For a given real wave vector $k = |\kappa_0|$, the square of the associated frequency, $\omega^2 Y_0^2/(gH_0)$, can be found minimising Rayleigh quotient

$$\frac{\int_{-1}^{1} dy \left[|\kappa_0|^2 Y_0^2 (1-y^2) f^2(y) + (1-y^2) \left(\frac{d}{dy} f(y) \right)^2 \right]}{\int_{-1}^{1} dy\, f^2(y)} \tag{26}$$

with respect to f. The variation of Rayleigh quotient (see (26)) around the minimising function, f_{κ_0}, leads to

$$\begin{aligned} &\frac{-\int_{-1}^{1} \left[|\kappa_0|^2 Y_0^2 (1-y^2) f_{\kappa_0}^2(y) + (1-y^2) \left(\frac{d}{dy} f_{\kappa_0}(y) \right)^2 \right] dy}{\left(\int_{-1}^{1} dy f_{\kappa_0}^2(y) \right)^2} \times \left[\int_{-1}^{1} dy f(y) \delta f(y) \right] \\ &\qquad + \frac{\left[|\kappa_0|^2 Y_0^2 (1-y^2) f_{\kappa_0}(y) - \frac{d}{dy} \left((1-y^2) \frac{d}{dy} f_{\kappa_0}(y) \right) \right] \delta f(y)}{\left(\int_{-1}^{1} dy f_{\kappa_0}^2(y) \right)} \end{aligned} \tag{27}$$

where the second term in the numerator of the last line has been obtained by integration by parts. No contribution comes from the bounds of the integral because f_{κ_0} is bounded at $y = \pm 1$. Noticing that f_{κ_0} minimises the Rayleigh quotient the first line of (27) is equal to $-\omega_0^2 (gH_0)^{-1} [\int_{-1}^{1} dy f_{\kappa_0}^2(y)]^{-1}$. Accordingly the variation becomes

$$\begin{aligned} &\frac{1}{\int_{-1}^{1} dy f_{\kappa_0}^2(y)} \\ &\times \int_{-1}^{1} dy \delta f(y) \left[-\frac{\omega_0^2 Y_0^2}{gH_0} f_{\kappa_0}(y) + |\kappa_0|^2 Y_0^2 (1-y^2) f_{\kappa_0}(y) - \frac{d}{dy} \left\{ (1-y^2) \frac{d}{dy} f_{\kappa_0}(y) \right\} \right] \end{aligned} \tag{28}$$

The variation must be zero for all variation δf since f_{κ_0} is minimising function. Therefore minimising function satisfies the ordinary differential equation given in (26). In [10] function f_{κ_0} was approximated by a polynomial of degree two. That is the reason of the *small* overestimation (see circles in Figure 3). When variation of η along y axis is ignored (f_{κ_0}:constant) the associated frequency is even higher (see stars in Figure 3). As mentioned earlier the strong dependence of the decaying modes on y coordinates can be observed in Figure 4. For a given $\omega = \sqrt{gH_0} k_{\text{inc}}^{\text{open}}$ the corresponding $\kappa^2 Y_0^2$ can be found minimising

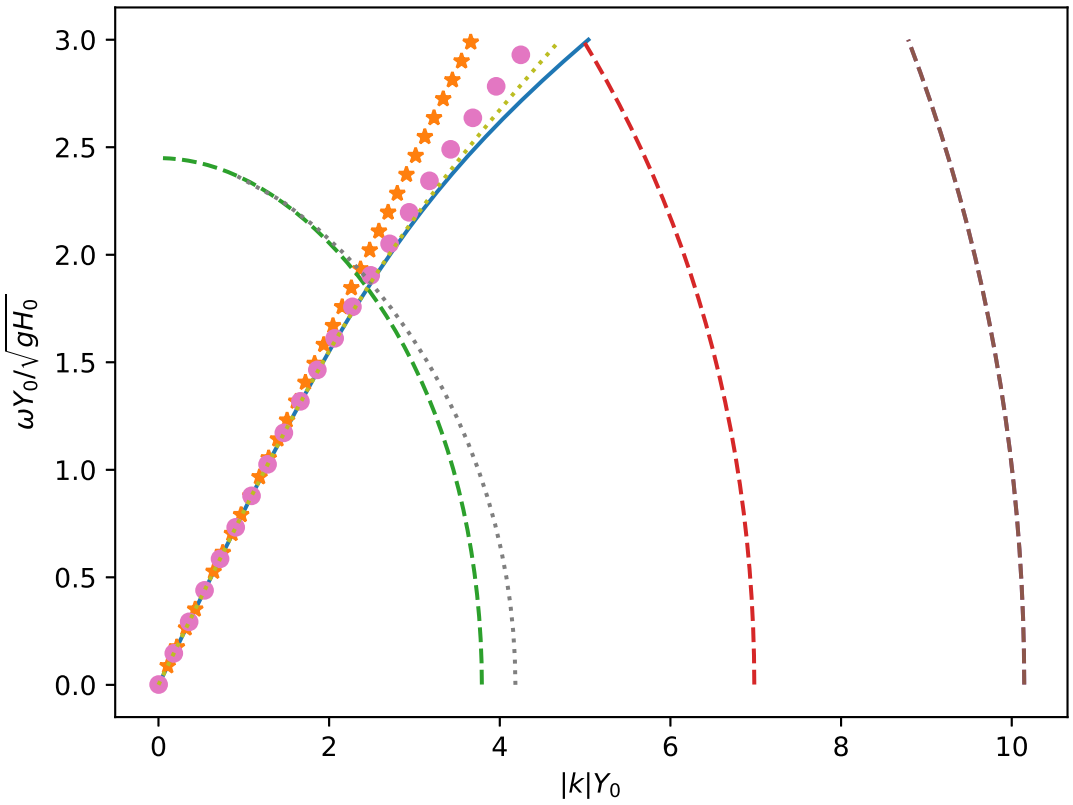

FIG. 3. The continuous and the broken curves are the dispersion relations for an infinite channel with parabolic cross section. Broken curves indicate a purely imaginary wave vector. The waves associated with such wave vectors decay exponentially in $-x$ direction because they are proportional to $\exp(|k|x)$. Continuous and broken curves were obtained using routine `eigh` (See Appendix). The equation of the bottom of the channel is $z = -H_0(1 - y^2/Y_0^2)$ where H_0 is its maximum depth and Y_0 is its half width. The stars are the dispersion relation given by $\omega = \sqrt{g2H_0/3}\,|k|$ where $2H_0/3$ is the average depth of the parabolic channel. The circles are the dispersion relation obtained using equation (2.51) from [10]. The dots (two branches) are the dispersion relation obtained from (32)

the following Rayleigh quotient

$$\frac{\int_{-1}^{1} dy \left[-\left(k_{\text{inc}}^{\text{open}} Y_0\right)^2 f^2(y) + (1-y^2)\left(\frac{d}{dy} f(y)\right)^2 \right]}{\int_{-1}^{1} dy\,(1-y^2) f^2(y)} \tag{29}$$

If trial f is restricted to a polynomial of degree 2 ($f(y) = A_0\sqrt{1/2} + A_2\sqrt{5/2}P_2(y)$) then

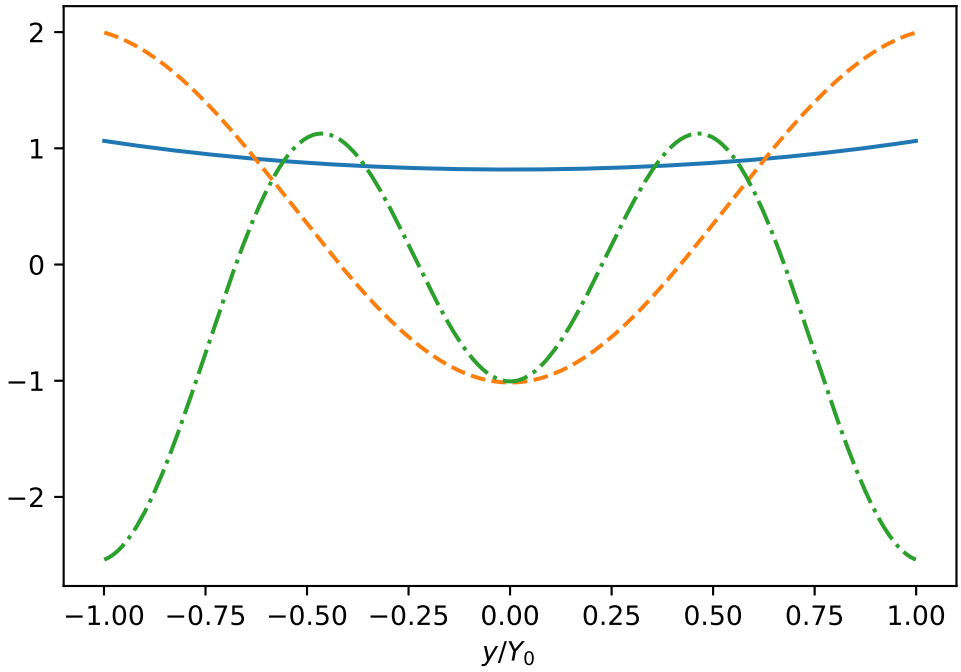

FIG. 4. The continuous curve represents the eigenfunction, $f_0(y,\omega)$, for $\omega Y_0/\sqrt{g\alpha x_0} = 1$. See equation 22 for the definition of f_{κ_0}. The dashed and the dash-dotted curves are respectively f_{κ_1} and f_{κ_2}. Function f_{κ_0} is associated with the oscillatory solution in x direction. Note that $f_{\kappa_0}(y)$ is almost constant.

Rayleigh quotient is

$$\frac{(A_0, A_2)\begin{pmatrix} -\left(k_{\text{inc}}^{\text{open}} Y_0\right)^2 & 0 \\ 0 & -\left(k_{\text{inc}}^{\text{open}} Y_0\right)^2 + 6 \end{pmatrix}\begin{pmatrix} A_0 \\ A_2 \end{pmatrix}}{(A_0, A_2)\begin{pmatrix} 0.666 & -0.298 \\ -0.298 & 0.476 \end{pmatrix}\begin{pmatrix} A_0 \\ A_2 \end{pmatrix}}. \tag{30}$$

The ratio above needs to be minimised with respect A_0 and A_2. At the minimising (A_0, A_2) the gradient of the denominator and numerator of the Rayleigh quotient must be parallel with the constant proportionality between the gradients being $(\kappa Y_0)^2$. There is a no trivial (A_0, A_2) that makes these gradients parallel if the determinant of the following matrix

vanishes

$$\mathrm{Det}\begin{bmatrix} \left(-(k_{\mathrm{inc}}^{\mathrm{open}})^2 - .6666\kappa^2\right) Y_0^2 & .2981(\kappa Y_0)^2 \\ .2981(\kappa Y_0)^2 & \left(-(k_{\mathrm{inc}}^{\mathrm{open}})^2 - .4762\kappa^2\right) Y_0^2 + 6 \end{bmatrix} = 0\,. \tag{31}$$

Solving the equation above, κ is obtained as a function of $\omega' = \omega Y_0/\sqrt{gH_0}$ as

$$|\kappa_{(0,1)}|Y_0 = \left| \sqrt{\frac{4 - 1.141286\omega'^2 - + \sqrt{(-4 + 1.141286\omega'^2)^2 - .91428(\omega'^4 - 6\omega'^2)}}{0.45714}} \right| \tag{32}$$

where $-+$ means - if subscript of κ is 0 (energy transmitting mode) and if the subscript is 1 then '+' is adopted (decaying mode). Two branches of the dispersion obtained from (32) is displayed as dots in Figure 3. The lower branch ($\omega = \omega(|\kappa_0|)$) obtained from (32) is more accurate than that given by equation(2.51) of [10](compare dotted curve and circles in Figure 3), however the difference between these two approximations become apparent only for frequencies larger than $\sqrt{6}\sqrt{gH_0}/Y_0$. This range of frequencies is beyond the scope of the present work as the decaying modes will cease to be decaying for this range.

There are two waves associated with purely imaginary κ_0 (power transmitting modes). One of this wave travel in the offshore direction the other in the opposite direction. The full solution in the vicinity of the mouth (inside the bay) can be written as

$$\eta_\omega(t, x', y') = \exp(i\omega t)\Bigg[\left\{ B_0^+ \exp(i|\kappa_0|x) + B_0^- \exp\left((-i|\kappa_0|x)\right\} f_{\kappa_0}(y') + \sum_{n=1}^{M-1} B_n \exp\left(|\kappa_n|(x - x_0)\right) f_{\kappa_n}(y') \Bigg]. \tag{33}$$

The solution above can be extended to the whole of the inclined bay using the fact that the phase difference,at a given instant, between two points separated by dx is $\pm|\kappa_0|\sqrt{x_0/x}dx$. Here the sign depends on the direction of travel of the wave. Integrating the argument of the exponential functions in the curly parenthesis (equation 33) from x_0 to x and multiplying the travelling wave by an appropriate factor to ensure conservation of energy (see (11)) η is found to be

$$\eta_\omega(t, x, y') = \exp(i\omega t)\Bigg[\sqrt{\frac{x_0}{x}} \Big\{ B_0^+ \exp\left(2i|\kappa_0|\sqrt{x_0 x}\,\right) + B_0^- \exp\left(-2i|\kappa_0|\sqrt{x_0 x}\,\right) \Big\} f_{\kappa_0}(y') + \sum_{n=1}^{M-1} B_n \exp\left(|\kappa_n|(x - x_0)\right) f_{\kappa_n}(y') \Bigg]. \tag{34}$$

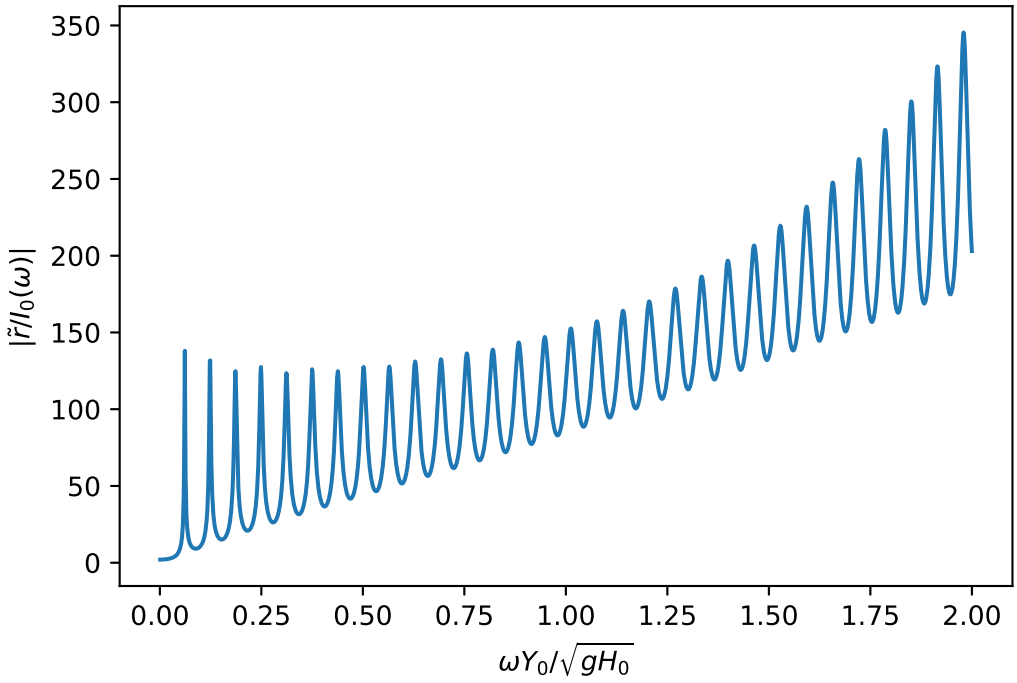

FIG. 5. Absolute value of Fourier transform of runup divided by that of the incident wave is displayed as function of the non dimensional frequence, $\omega Y_0/\sqrt{gH_0}$. The length of the inclined parabolic channel is $x_0 = 10Y_0$(Y_0 is half width at the mouth of the bay)

Again the boundary condition at the inland tip of the bay requires that $B_0^+ = -B_0^-$. The decaying waves never reach $x = 0$ because $|\kappa_n| \gg 1/x_0$ for $n = 1, 2, .., M-1$. Taking into account the boundary condition at the tip (34) is reduced to

$$\eta_\omega(t, x, y') = \exp(i\omega t)\left[B_0^* j_0(2|\kappa_0|\sqrt{x_0 x}) f_{\kappa_0}(y') + \sum_{n=1}^{M} B_n \exp\left(|\kappa_n|(x - x_0)\right) f_{\kappa_n}(y')\right] \quad (35)$$

where spherical Bessel function $j_0(z)$ is $\sin(z)/z = \sqrt{\frac{\pi}{2z}} J_{1/2}(z)$. Here $J_{1/2}$ is Bessel function of fractional order. In the vicinity of the inland tip of the bay the right hand side of (35) is not rigorous solution of LSW unless one makes the approximations $|\kappa_0| \approx \omega/\sqrt{g\frac{2}{3}H_0}$(see stars and continuous curve in figure 3), $f_{\kappa_0} \approx 1$ (see the continuous curve in figure 4) and $\exp\left(|\kappa_n|(x - x_0)\right) = 0$ for $n = 1, 2..M-1$. Coefficients $B_0^*(\omega), B_1(\omega), B_2(\omega), ...B_{M-1}(\omega)$ will be found from the boundary conditions at the entrance of the bay.

The solution of LSW for a monochromatic incident wave in the open sea is the scattered wave by the mouth added to the sum of incident and reflected waves. If there were no bay

all the incident wave would be reflected by the coast line at $x = x_0$. In the open sea the scattered field can be seen as a disturbance due to the presence of the bay. In the first part we use Dirichlet condition because the scattered field was assumed to be much smaller than reflected/incident wave. The scattered field is generated by a virtual source distribution $s_\omega(t, y) = \tilde{s}(\omega, y)\exp(i\omega t)$ at the entrance of the bay ($x = x_0$, $-Y_0 < y < Y_0$). A unit discharge $\exp(i\omega t)$ into the open sea concentrated at $x = x_0, y = y^*$ with $-Y_0 < y^* < Y_0$ will generate a free surface disturbance

$$\frac{\omega}{2gH_0}\mathrm{H}_0^{(2)}\left(\frac{\omega}{\sqrt{gH_0}}|\mathbf{r} - x_0\hat{\mathbf{i}} - y^*\hat{\mathbf{j}}|\right)\exp(i\omega t)$$

at position $\mathbf{r}$. Here $\mathrm{H}_0^{(2)}$ is Hankel fuction with $\mathrm{H}_0^{(2)}(z)$ proportional to $\exp(-iz)$ for large z. Thus this Hankel function multiplied by $\exp(i\omega t)$ represents a wave propagating in the outward direction. For small argument logarithmic approximation ($\mathrm{H}_0^{(2)}(z) \approx (-2i/\pi)\ln(z)$) may be used. Accordingly, in the near field depth integrated velocity $H_0\mathbf{v}$ associated with the free surface disturbance above becomes according to [11], page 194

$$\frac{1}{\pi d}\hat{\mathbf{n}}\exp(i\omega t)$$

using $\partial_t\mathbf{v} = -g\mathbf{grad}\eta$. Here d is the distance to the discharge and $\hat{\mathbf{n}}$ is the outward unit vector ($\hat{\mathbf{n}}$ is in the direction of the vector connecting the position of the concentrated discharge to $\mathbf{r}$). The flux generated by the above depth integrated fluid velocity into the open sea is $\exp(i\omega t)$ according to [11]. The full wave in the open

$$\eta_\omega^{\mathrm{open}}(t, x, y) = \left[\frac{\omega}{2gH_0}\int_{-Y_0}^{Y_0} dy^*\,\tilde{s}(\omega, y)\mathrm{H}_0^{(2)}\left(\frac{\omega}{\sqrt{gH_0}}|\mathbf{r} - x_0\hat{\mathbf{i}} - y^*\hat{\mathbf{j}}|\right)\exp(i\omega t)\right] \qquad (36)$$
$$+2I_0(\omega)\cos\left(\frac{\omega}{\sqrt{gH_0}}(x - x_0)\right)\exp(i\omega t)$$

where the source distribution $\tilde{s}(\omega, y)$ is equal to

$$-H_0(1 - (y/Y_0)^2)\frac{g}{i\omega}\frac{\partial}{\partial x}\,\eta(t, x)|_{x=x_0^-} \qquad (37)$$

because of the continuity of the depth integrated flow in x direction across the boundary. With the help of the equation above $\tilde{s}(\omega, y)$ becomes a function of constants $B_0^*(\omega), B_1(\omega), .., B_{M-1}(\omega)$. The water level according to (36) is also a function of $B_0^*(\omega), B_1(\omega), .., B_M(\omega)$. These constants will be chosen to minimise the penalty integral

$$\int_{-Y_0}^{Y_0} dy\,\left|\tilde{\eta}^{\mathrm{open}}(\omega, x_0^+, y) - \tilde{\eta}(\omega, x_0^-, y)\right|^2 \qquad (38)$$

where $\tilde{\eta}(\omega, x, y) = \eta_\omega(t, x, y)\exp(-i\omega t)$ is independent of time. In the same way $\tilde{\eta}^{\text{open}}(\omega, x_0^+, y)$ is also independent of time. With the help of the Gauss quadrature the penalty integral can be transformed to finite summation

$$\sum_{n=1}^{N} w_n \left|\tilde{\eta}^{\text{open}}(\omega, x_0^+, y_n) - \tilde{\eta}(\omega, x_0^-, y_n)\right|^2 \tag{39}$$

with $N > M$. Here w_n's and y_n's are weights and knots of the the Gauss quadrature. The least square solution of the over determined system of equations below

$$\sqrt{w_n}\tilde{\eta}(\omega, x_0^-, y_n, B_0^*, B_1, .., B_{M-1}) = \sqrt{w_n}\tilde{\eta}^{\text{open}}(\omega, x_0^+, y_n, B_0^*, B_1, .., B_{M-1}) \tag{40}$$

with $n = 0, 1, , .., N-1$ leads to $B_0^*, B_1, .., B_{M-1}$ that minimises the summation given by (39)(see [7]). In obtaining $\tilde{\eta}^{\text{open}}(\omega, x_0, y)$ as a linear function of $B_0^*, B_1, .., B_{M-1}$ Hankel function with logarithmic singularity needs to be integrated with respect to y. In the vicinity the singularity, Hankel function divided by log function has been approximated by a polynomial then this polynomial multiplied by log function is integrated analytically. Once the constants $B_0^*, .., B_{M-1}$ are known the linear runup is obtained as $r_\omega(t) = B_0^*(\omega)\exp(i\omega t)$ because in the series given (35), spherical Bessel function is 1 for $x = 0$. In figure 5 the amplitude of runup $r_\omega(t)$ is displayed as a function of the incident wave frequency, (amplitude of the incident wave is normalised to unity). Sharps peaks in that figure indicate that the poles of $\tilde{r}(\omega) = r_\omega(t)\exp(-i\omega t)$ in the complex ω plane are close to the real axis. The closeness of these poles to the real ω axis will be responsible of the effective trapping of energy of the wave inside the bay.

The general trend in figure 5 is that $\tilde{r}(\omega) \propto \omega^1$. This is in agreement with the predictions of (14) where for a given frequency and depth the runup was proportional to the length of the bay. Note that an important no dimensional parameter that controls amplification (ratio between the amplitude of the runup and that of incident wave) is the length of the bay divided by the wavelength of incident wave. On a sloping beach the runup is proportional to $\omega^{1/2} I_0$ where I_0 is the amplitude of the incident wave at a distance L from the coast (see [12]). In the case of a converging bay the amplification of short waves is more effective because of the focusing the energy of the wave to the inland tip of the bay.

In this section it was assumed the incident wave is in the the form $I_0(\omega)\exp(i\omega(t + x/\sqrt{gH_0})$ (see (36)). For an incident wave train one should then integrate $r_\omega(t) =$

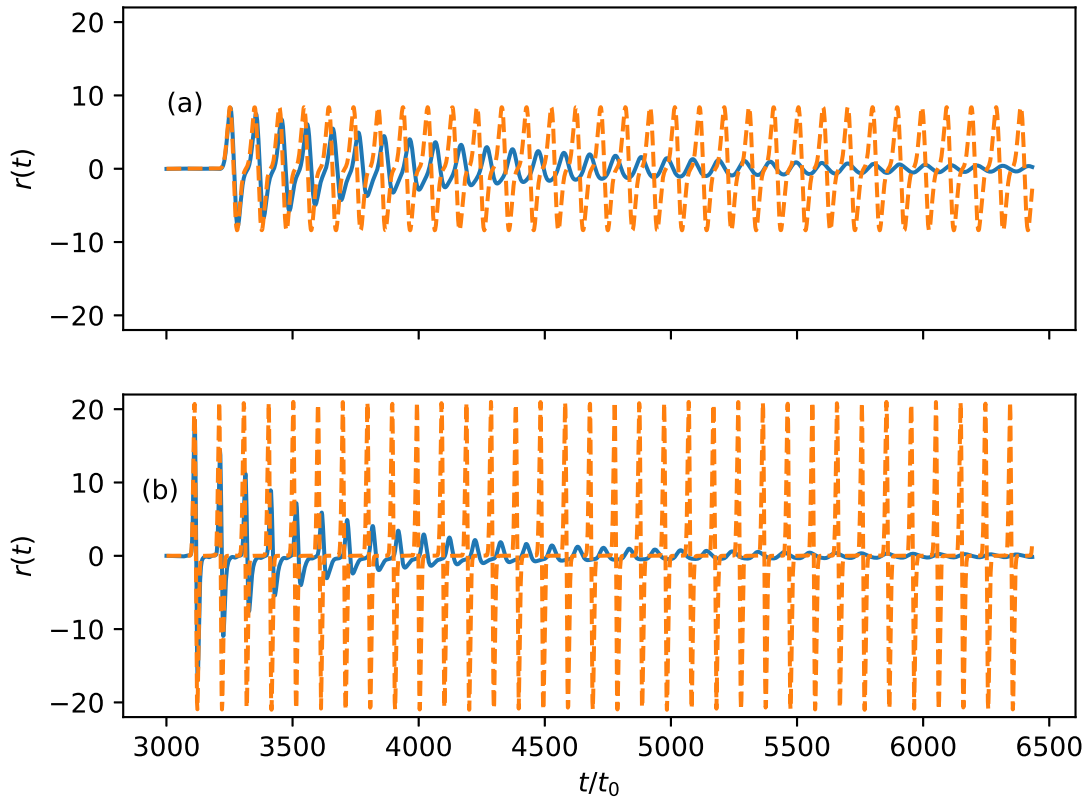

FIG. 6. Continuous curves are runup for an incident Gaussian waves . In Figure (a) the incident wave in the open sea is exp $\left(-(x+\sqrt{gH_0}(t-T/2)-x_0)^2 x_0^{-2}\right)$ and in Figure(b) narrower Gaussian is given by exp $\left(-(x+\sqrt{gH_0}(t-T/2)-x_0)^2(0.4x_0)^{-2}\right)$. Ratio $x_0/(2Y_0)$ is 10. Here x_0 is the length of the bay and $2Y_0 = 2\sqrt{\alpha x_0 y_0}$ is the width of the mouth of the bay (see (8) for the geometry of the bay). Time scale t_0 is given by $Y_0/\sqrt{gH_0}$. The broken curves are the runup associated with Dirichlet problem $\eta(t, x_0^-) = 2\eta_{\rm inc}^{\rm open}(t, x_0^+)$ (see (6)). Parameter T is duration of the sampling of the incident wave. The solution associated Dirichlet boundary condition over estimates the maximum runup by 1% in (a) and 12% in (b). The solutions associated with Dirichlet boundary conditions are not damped. Note that two ways travelling time along this bay is $97.98\, t_0 = 2\sqrt{6}\, x_0/\sqrt{gH_0}$

$\tilde{r}(\omega)\exp(i\omega t)$ over the frequencies in order to obtain $r(t)$. Function

$$I_0(\omega) = \frac{1}{2\pi}\int_{-\infty}^{\infty} dt\, \eta_{\rm inc}^{\rm open}(t, x_0^+)\exp(-i\omega t)$$

is the Fourier transform of the incident wave train at $x = x_0^+$. Fourier transform of $\eta_{\rm open}^{\rm inc}$ and inverse Fourier transform of $\tilde{r}(\omega)$ has been carried out using Fast Fourier routines

from `Python, numpy package`. Discrete Fourier transform introduces inevitably an artificial periodicity of the input signal. The incident wave train has been sampled over such long period that this periodicity does not affect the runup. The modes in the bay excited by the incident wave die completely (due to the radiation damping) before the next incident wave train arrives (see Figure 6). Function $\tilde{r}(\omega)$ has been evaluated at discrete frequency ranging between 0 and Nyquist frequency. In this range, the argument of Hankel function in (36) remains positive. For negative frequencies reality condition has been used ($\tilde{r}(-\omega)$ is complex conjugate of $\tilde{r}(\omega)$). In Figure 6 two Guaussian incident wave packets of different widths ($\eta_{\text{inc}}^{\text{open}} = \exp\left(-(x+\sqrt{gH_0}(t-T/2)-x_0)^2 L_{(a,b)}^{-2}\right)$) are considered here where $L_{(a,b)}$ is x_0 in top plot (a) and $0.4x_0$ in bottom plot (b). Parameter T is duration of the sampling. The continuous curves are associated with the solution of obtained from (40) where $r(t)$ is the inverse Fourier transform of $\tilde{r} = B_0^*(\omega)$. The broken curves are runups from (14)(Dirichlet boundary condition). The solution associated Dirichlet boundary condition overestimates the maximum runup by 1% in (a) and 12% in (b). In the introduction it was mentioned that the Dirichlet boundary condition is an accurate approximation of real boundary conditions for $\omega \ll \sqrt{gH_0}/Y_0$. That is why the predictions of (14) overestimates the maximum runup by higher margin in Figure 6(b) where shorter wavelengths are involved. According to the approximate power law $\tilde{r}(\omega) \propto \omega^1$ on would have expected the ratio between maximum runups in (a) and (b) in Figure 6 to be 2.5 . It turns out the actual value of this ratio is 2.2 (this ratio obtained from (14) is exactly 2.5). Failure of the relation, $r \propto \omega$, is due to the fact that the short waves 'see' broaden peaks in Figure 5. With increasing frequencies the poles of $\tilde{r}(\omega)$ move away from the real ω axis making the peaks at the right side of Figure 5 broader. The rapid decay of oscillations in figure 6(b) is due to the fact that narrower Gaussian excites modes with shorter wavelengths. The complex frequencies of homogeneous solutions of LSW in the bay are the poles of $\tilde{r}(\omega)$ in the complex ω plane. The homogeneous solutions with shorter wavelengths are associated with poles that are related to peaks at the right side of Figure 5. Therefore they decay quickly transmitting their energy to the open sea.

IV. PERTURBATION OF DIRICHLET BOUNDARY CONDITION

Dirichlet boundary condition condition ($\eta(t,x_0^-)=2\eta_{\rm inc}^{\rm open}(t,x_0^+)$) leads to solutions that tend overestimate the maximum runup because the sea level perturbation at $x=x_0^+$ is less then $2\eta_{\rm inc}^{\rm open}(t,x_0^+)$). This is due to partial penetration of the incident wave inside the bay. A perturbative approach will be adopted where only one dimensional solutions of the wave equation inside the bay will be required. Dirichlet boundary condition is not 'exact' because it violates the continuity of the depth integrated x velocity across the mouth of the bay. When scattered field into the open sea is ignored depth integrated velocity is zero at $x=x_0^+$ but the sea level perturbation, $2\eta_{\rm inc}^{\rm open}(t,x_0^+)$, will trigger a wave progressing toward the inland tip of the bay. The simple relation between u and η for a wave progressing in $-x$ direction is $u=-\sqrt{g/\bar{H}(x)}\,\eta$. Because of the continuity of η at $x=x_0$ the depth integrated velocity associated with this progressive wave at the entrance of the bay is

$$H(x_0^-,y)u^{(0)}(t,x_0^-)=-2H(x_0^-,y)\sqrt{g/\bar{H}(x_0^-)}\,\eta_{\rm inc}^{\rm open}(t,x_0^+) \tag{41}$$

All quantities relating to the undisturbed Dirichlet condition will be referred with superscript $^{(0)}$. A distribution of sources

$$s^{(1)}(t,y)=2u^{(0)}(t,x_0^-)H(x_0,y) \tag{42}$$

placed at the entrance of the bay the will ensure the continuity of depth integrated velocity. Factor 2 in the above equation is due to the fact that this source distribution is forced to generate waves that progress only toward the open sea. The superscript ^{1} was used because sources $s^{(1)}$ will generate a scattered field $\eta_{\rm open}^{(1)}(t,x,y)$ in the open sea that will disturb the boundary condition $\eta(t,x_0^-)=2\eta_{\rm inc}^{\rm open}(t,x_0^+)$. Evidently $\eta_{\rm open}^{(1)}(t,x,y)$ will be a two dimensional field depending strongly y coordinate. It will be shown that $\eta_{\rm open}^{(1)}(t,x,y)$ is of order of $(\omega Y_0/\sqrt{gH_0})\eta_{\rm inc}^{\rm open}(t,x_0^+)$ within the relevant time range. In principle $\eta^{(1)}(t,x,y)$ must be continuous across the entrance of the bay but because $\eta^{(1)}(t,x,y)\ll\eta_{\rm inc}^{\rm open}(t,x,y)$ this condition can be replaced by a less stringent one,

$$\eta^{(1)}(t,x_0^-)=\bar{\eta}_{\rm open}^{(1)}(t,x_0^+)=\frac{1}{2Y_0}\int_{-Y_0}^{Y_0}dy\,\eta_{\rm open}^{(1)}(t,x_0^+,y)\,. \tag{43}$$

This simplification renders the problem one dimensional within the inclined bay. The solution of the Dirichlet problem is

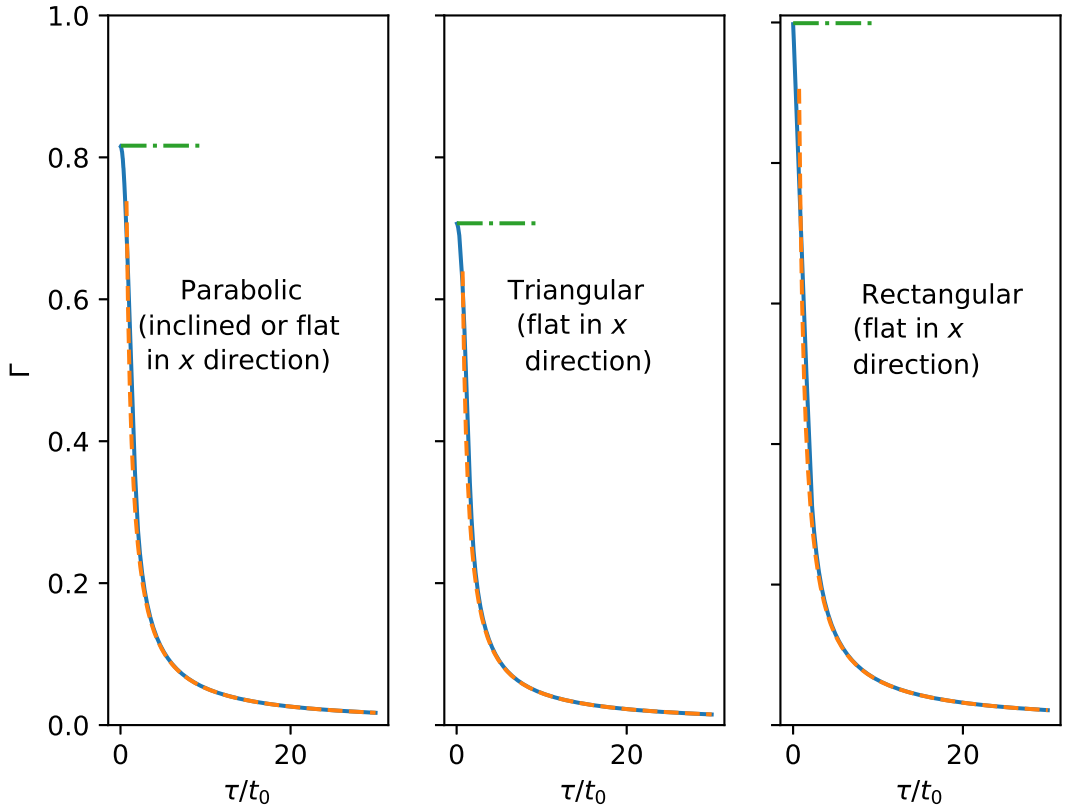

FIG. 7. The continuous curves are function $\Gamma(\tau)$ displayed as a function of non dimensional time τ/t_0 with $t_0 = Y_0/\sqrt{gH_0}$. See (59) for the definition of Γ. The horizontal dot dashed lines are $\sqrt{< H >/H_0}$(see (62)). The dashed curves are asymptotic approximation given by (63) . For triangular bay the depth is $H(y) = H_0(1 - |y|/Y_0)$ (depth independent of x) . For rectangular bay the depth is uniform with $H = H_0$.

$$\eta^{(1)}(t,x) = \sqrt{\frac{x_0}{x}}\left[\bar{\eta}^{(1)}\left(t - \frac{\sqrt{6x_0}(\sqrt{x_0}-\sqrt{x})}{\sqrt{gH_0}}, x_0^+\right) - \bar{\eta}^{(1)}\left(t - \frac{\sqrt{6x_0}(\sqrt{x_0}+\sqrt{x})}{\sqrt{gH_0}}, x_0^+\right)\right] \quad \text{for} \quad 0 < x < x_0 \tag{44}$$

where the second line of the equation above represents the wave reflected by the inland tip of the bay. Note that any function of $t \pm \sqrt{6x/(g\alpha)}$ is a solution of laterally averaged LSW. Equation (44) will be valid as long as the waves reflected by the inland tip do not reach the entrance of the bay because the relation given by (41) holds only for waves progressing in $-x$ direction.

The free surface perturbation $\eta^{(1)}(t,x)$ generates its own flow $u^{(1)}$ that will perturb the flux continuity at $x = x_0$. The same procedure needs to be repeated with $s^{(2)}$. The full iterative solution can be written as

$$\begin{aligned} s(t,y) &= s^{(1)}(t,y) + s^{(2)}(t,y) + ... \\ \eta(t,x) &= \eta^{(0)}(t,x) + \eta^{(1)}(t,x) + \eta^{(2)}(t,x) + ... \end{aligned} \tag{45}$$

It will be shown that the series above converge rapidly if the relative variation of the incident wave within the time scale, $t_0 = Y_0/\sqrt{gH_0}$ is small. This will be the case if the characteristic wavelength of the incident wave is much larger the width of the bay.

The contribution from $\eta^{(i)}(t,x)$ to the runup will be

$$r^{(i)}(t) = 4x_0\sqrt{\frac{6}{gH_0}}\frac{\partial}{\partial t}\eta^{(i)}\left(\sqrt{gH_0}\left(t - x_0\sqrt{\frac{6}{H_0 g}}\right), x_0^-\right) \tag{46}$$

according to (14).

We will now show how explicitly $\eta^{(i)}(t, x_0^+)$ can be written as a function of $s^{(i)}(t', y)$ for $t > t'$. Let $g_r(t, x, y, t', x', y')$ be the retarded free surface response to a sudden fluid incursion of unit volume into two dimensional infinite sea at instant t' and at a position (x', y'). Function g_r will then satisfy the inhomogeneous equation,

$$\left[\frac{\partial^2}{\partial t^2} - gH_0\left(\frac{\partial^2}{\partial x^2} + \frac{\partial^2}{\partial y^2}\right)\right] g_r = \delta(x - x')\delta(y - y')\frac{d}{dt}\delta(t - t')\,. \tag{47}$$

To solve this for $t \to t'^+$, it is sufficient to integrate the right side of the equation above twice with respect to t. Note that the term, $\partial_{xx} + \partial_{yy}$, can be ignored because the waves will not have enough time to travel. This integration leads to

$$\left.\frac{\partial}{\partial t} g_r\right|_{t=t'^+} = 0, \quad \text{and} \quad g_r = \delta(x - x')\delta(y - y') \tag{48}$$

for $t \to t'^+$. Therefore initial fluid velocity $\mathbf{v}$ vanishes because $H_0 \mathrm{div}\,(\mathbf{v})$ is $-\partial_t g_r$. The vanishing initial velocity ensures the integral ,

$$\int_{-\infty}^{\infty} dx \int_{-\infty}^{\infty} dy g_r(t, x, y, x', y')\,, \tag{49}$$

will be independent of time for $t > t'$. Further more the integral of g_r, $\int^t dt'' g_r(t'', x, y, t', x', y')$ is the usual retarded green function associated with D'Alambertian operator in two dimensions $(\partial_{tt} - gH_0[\partial_{xx} + \partial_{yy}])$. Thus function g_r is (see [17] page 235)

$$\frac{1}{2\pi\sqrt{gH_0}}\frac{\partial}{\partial t}\left(\frac{\theta\left(gH_0(t-t')^2 - (x-x')^2 - (y-y')^2\right)}{\sqrt{gH_0(t-t')^2 - (x-x')^2 - (y-y')^2}}\right). \tag{50}$$

where θ is the step function. To compute $\eta^{(i)}$ for $x = x_0^+$, one should proceed to convolution of $s^{(1)}$ with g_r given in (50). In this convolution x and x' will be equal to x_0 and $\eta^{(i)}$ will be obtained as

$$\eta^{(i)}(t, x_0^+, y) = \int_{-\infty}^{t} dt' \int_{-Y_0}^{Y_0} dy' \frac{s^{(i)}(t', y')}{2\pi\sqrt{gH_0}} \frac{\partial}{\partial t} \left(\frac{\theta\left(gH_0(t-t')^2 - (y-y')^2\right)}{\sqrt{gH_0(t-t')^2 - (y-y')^2}} \right). \tag{51}$$

Inspecting the integral above one notices that if the time dependence of $s^{(i)}(t', y)$ is $\theta(t')$ then the integration with respect to t' can be carried out and $\eta^{(i)}$ becomes proportional to

$$\frac{1}{\sqrt{gH_0 t^2 - (y-y')^2}}\,.$$

Thus $\eta^{(i)}$ decays quickly for $t \gg Y_0/\sqrt{gH_0}$. To sustain $\eta^{(i)}(t, x_0^+, y)$ the source, $s^{(i)}(t', y)$, must vary with time. According to the dimensional analysis $\eta^{(i)}(t, x_0^+, y)$ is of order of

$$\frac{1}{\sqrt{gH_0}} t_0 \frac{\partial}{\partial t'} s^{(i)}(t', y')$$

where t_0 is $Y_0/\sqrt{gH_0}$. Taking into account $s^{(i)} \propto \sqrt{gH_0}\eta^{(i-1)}$, the proportionality relation

$$\eta^{(i)} \propto \underbrace{\left(\frac{Y_0}{\sqrt{gH_0}} \right)}_{t_0} \frac{\partial}{\partial t} \eta^{(i-1)} \tag{52}$$

is obtained. Therefore the series given by (45) converges rapidly if the period of the incident wave is much larger than $t_0 = Y_0/\sqrt{gH_0}$.

The averaged value of $\eta^{(i)}(t, x_0^+, y)$ across the width of the bay is

$$\bar{\eta}^{(i)}(t, x_0^+) = \frac{1}{2Y_0} \Bigg[$$

$$\int_{-Y_0}^{Y_0} dy \int_{-\infty}^{t} dt' \int_{-Y_0}^{Y_0} dy' \frac{s^{(i)}(t', y')}{2\pi\sqrt{gH_0}} \frac{\partial}{\partial t} \left(\frac{\theta\left(gH_0(t-t')^2 - (y-y')^2\right)}{\sqrt{gH_0(t-t')^2 - (y-y')^2}} \right) \Bigg]. \tag{53}$$

If the radius of the causality circle ($\sqrt{gH_0}(t-t')$) is less than $2Y_0$ then the integrand in the equation above will have severe discontinuity within the domain of integration. In general the source term ,

$$s^{(i)}(t', y')\,,$$

is smoother function than

$$\frac{\partial}{\partial t} \left(\frac{\theta\left(gH_0(t-t')^2 - (y-y')^2\right)}{\sqrt{gH_0(t-t')^2 - (y-y')^2}} \right).$$

Therefore it is preferable to proceed to the integration by part in (53) with respect to integration variable dt'. The integration by part leads to

$$\bar{\eta}^{(1)}(t,x_0^+) = \frac{1}{2Y_0}\Bigg[\int_{-Y_0}^{Y_0} dy \int_{-\infty}^{t} dt' \int_{-Y_0}^{Y_0} dy' \frac{\frac{\partial}{\partial t'} s^{(1)}(t',y')}{2\pi\sqrt{gH_0}} \left(\frac{\theta\left(gH_0(t-t')^2 - (y-y')^2\right)}{\sqrt{gH_0(t-t')^2 - (y-y')^2}} \right) \Bigg]. \tag{54}$$

where the identity,

$$\frac{\partial}{\partial t} g_r(t,x,y,t',x',y') = -\frac{\partial}{\partial t'} g_r(t,x,y,t',x',y'),$$

has been taken into account. Interchanging the order of integration in (54), this equation becomes

$$\bar{\eta}^{(i)}(t,x_0^+) = \frac{1}{2Y_0}\Bigg[\int_{-\infty}^{t} dt' \int_{-Y_0}^{Y_0} dy' \int_{-Y_0}^{Y_0} dy \frac{\frac{\partial}{\partial t'} s^{(i)}(t',y')}{2\pi\sqrt{gH_0}} \left(\frac{\theta\left(gH_0(t-t')^2 - (y-y')^2\right)}{\sqrt{gH_0(t-t')^2 - (y-y')^2}} \right) \Bigg]. \tag{55}$$

Now the analytical integration with respect to y yields

$$\bar{\eta}^{(i)}(t,x_0^+) = \frac{1}{2Y_0}\Bigg[\int_{-\infty}^{t} dt' \int_{-Y_0}^{Y_0} dy' \frac{\frac{\partial}{\partial t'} s^{(i)}(t',y')}{2\pi\sqrt{gH_0}} \Bigg(\arcsin\left(\min(1, \frac{Y_0 - y'}{\sqrt{gH_0}t}) \right) + \arcsin\left(\min(1, \frac{|-Y_0 - y'|}{\sqrt{gH_0}t}) \right) \Bigg) \Bigg]. \tag{56}$$

Source term $s^{(i)}$ can be eliminated from equation above using

$$\begin{aligned} s^{(i)}(t,y') &= 2H(x_0,y')u^{(i-1)}(t,x_0^-) = \\ &= -2H(x_0,y')\sqrt{\frac{g}{\bar{H}(x_0)}}\eta^{(i-1)}(t,x_0^-) \end{aligned} \tag{57}$$

and the sea level averaged at the mouth of the bay can be cast in the form

$$\bar{\eta}^{(i)}(t,x_0^+) = -\int_0^{+\infty} d\tau \frac{\partial}{\partial t} \eta^{(i-1)}(t-\tau, x_0^-)\Gamma(\tau) \tag{58}$$

where

$$\Gamma(\tau) = \frac{1}{2\pi\bar{H}(x_0)Y_0} \int_{-Y_0}^{Y_0} dy'\, H(x_0,y') \Bigg[\arcsin\left(\min(1, \frac{Y_0 - y'}{\sqrt{gH_0}\tau}) \right) + \arcsin\left(\min(1, \frac{|-Y_0 - y'|}{\sqrt{gH_0}\tau}) \right) \Bigg]. \tag{59}$$

The value of $\bar{H}(x_0)$ is $2H_0/3$ for parabolic bay. The computation of Γ will be repeated for bays with triangular and rectangular cross section where $\bar{H}$ is $H_0/2$ and H_0 respectively. These triangular and rectangular bays will have uniform depth in the longitudinal (x) direction. Otherwise these bays will not be non-reflecting. Functions $\Gamma(t)$ for various geometries are displayed in Figure(7).

If the incident wave in the open sea is a step function given by

$$\theta\left(\sqrt{gH_0}t + (x - x_0)\right)$$

then $\eta^{(0)} + \eta^{(1)}$ at $x = x_0^+$ averaged over the width of the bay will be

$$2\left(1 - \Gamma(t)\right) . \tag{60}$$

In the early and late stages of the diffraction simple approximations of function $\Gamma(t)$ can be found for semi-infinite channels of arbitrary cross section. The source distribution at the mouth of the semi-infinite channel for an incident step function is

$$s^{(1)}(y) = 2u^{(0)}H(y) = -4\sqrt{\frac{g}{\bar{H}}}H(y) .$$

At the early stage of the generation of waves by the source distribution above, the geometrical spreading of the waves in the open sea remains negligible. The solution of the one dimensional wave equation ($\partial_{tt}\eta - gH_0\partial_{xx}\eta = 0$) for those generated by $s^{(1)}(y)$ is then

$$-2\sqrt{\frac{1}{\bar{H}H_0}}H(y)\theta\left(\sqrt{gH_0}\,t - (x - x_0)\right) . \tag{61}$$

Averaging the equation above for $x = x_0$ across the channel and multiplying the average by $-1/2$ (see (60))

$$\Gamma(t) \approx \sqrt{\frac{\bar{H}}{H_0}} = \begin{cases} \sqrt{2/3} & \text{parabolic channel} \\ \sqrt{1/2} & \text{triangular channel} \\ 1 & \text{rectangular channel} \end{cases} \tag{62}$$

is obtained in the limit $t \ll W/\sqrt{gH_0}$ (here W is the width of the channel). In the opposite limit $t \gg W/\sqrt{gH_0}$ green function function $G(t, x, y, t', x', y')$ can be approximated by

$$G(t, x, y, t', x', y') \approx \frac{1}{2\pi g H_0}\frac{\partial}{\partial t}\left(\frac{1}{|t - t'|}\right) .$$

Proceeding to convolution of the green function above with the sources associated with the incident step function

$$\Gamma(t) \approx \frac{W}{\pi H_0}\sqrt{\frac{\bar{H}}{g}}\,\frac{1}{t} \tag{63}$$

is found for $t \gg W/\sqrt{gH_0}$. Function $\Gamma(t)$ together with these asymptotic approximations is displayed for 3 different geometries in figure (7)

A. A wave train entering a rectangular bay of uniform depth

Another example of no-reflecting bay is a rectangular bay of uniform depth. For such rectangular bays the time periodical solutions of shallow water equation inside the bay are given by

$$\eta = \int_0^\infty d\omega\, B_0(\omega)\cos\left(\frac{\omega}{\sqrt{gH_0}}x\right)\exp(i\omega t) \tag{64}$$
$$+\sum_{n=1}^{N} B_n(\omega)\exp\left(\sqrt{gH_0|\kappa_n|^2-\omega^2}\,(x-x_0)/\sqrt{gH_0}\right)\cos(\kappa_n\, y)\exp(i\omega t) + \text{c.c.}$$

where κ_n is $n\pi/Y_0$ and c.c. denotes complex conjugate. The distribution of virtual sources, $\tilde{s}(\omega, y)$, at the mouth of bay is equal to $2H_0 g\partial_x\tilde{\eta}(\omega, x_0^-, y)/(i\omega)$ because of the continuity of depth integrated velocities. Here $\tilde{\eta}$ is the Fourier transform of η with respect to time. Therefore the scattered field into open sea is a functions of coefficients $[B_k(\omega)]_{k=0}^N$ in (64). The continuity of η across the mouth of the bay provide a set of over determined equations that can be solved applying (38). When the Dirichlet condition $\eta(t, x_0^-) = 2\eta_{\text{inc}}^{\text{open}}(t, x_0^+)$ is used, the amplitude of the transmitted wave into the bay becomes twice of that of the incident wave with

$$\eta_{\text{transmitted}}(t, x) = 2\eta_{\text{inc}}^{\text{open}}(t - \frac{x_0 - x}{\sqrt{gH_0}}, x = x_0^+)\,.$$

The runup is the sum of the transmitted wave with that reflected by the inland tip of the bay. Accordingly the runup, $r^{(0)}(t)$ associated with Dirichlet boundary condition is

$$r^{(0)}(t) = 4\eta_{\text{inc}}^{\text{open}}(t - \frac{x_0}{\sqrt{gH_0}}, x = x_0^+)\,. \tag{65}$$

Factor 4 in the equation above can be clearly seen in figure 9 (see broken curve in that figure). When a gaussian a wave packet $\exp\left\{-\left(x + \sqrt{gH_0}[t - T/2]\right)/(0.4x_0)^2\right\}$ enters the

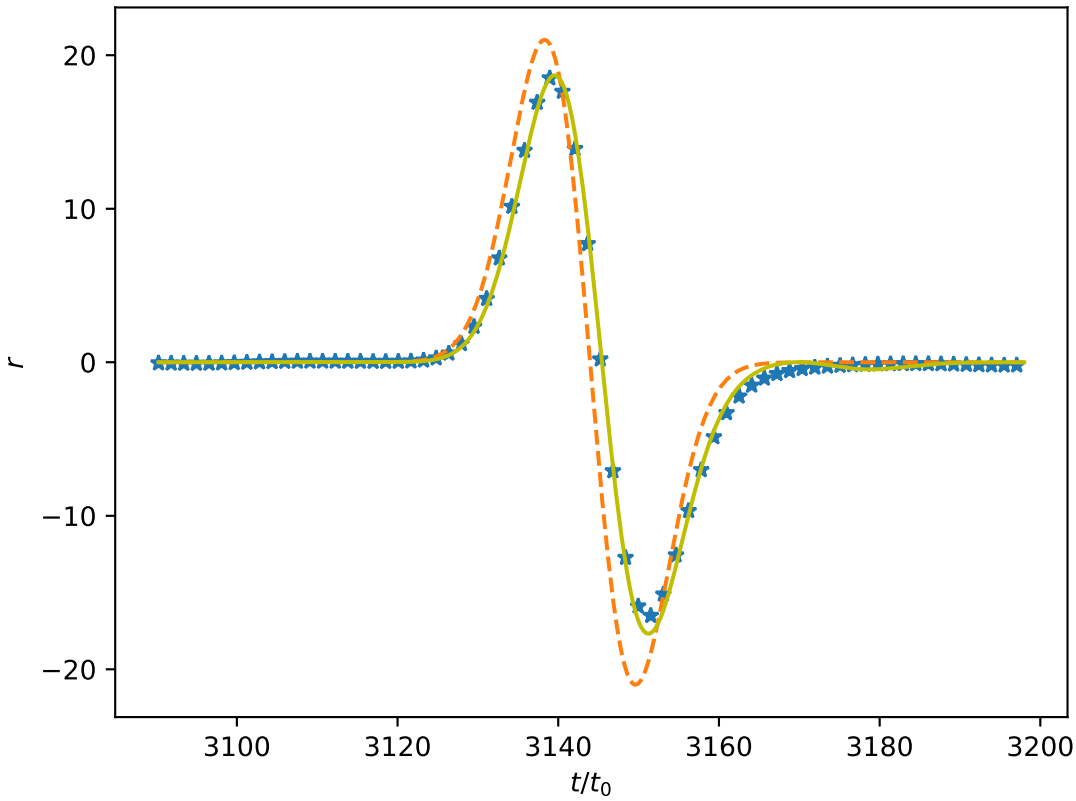

FIG. 8. Runup generated by a gaussian incident wave given by $\exp\left(-\left((x+\sqrt{gH_0}(t-T/2)/(0.4x_0)\right)^2\right)$ entering an inclined parabolic bay of aspect ratio $x_0/(2Y_0) = 10$. Continuous curve is the solution of integral equation, broken curve is $r^{(0)}(t)$ (undisturbed solution of Dirichlet problem), the stars are $r^{(0)}(t) + r^{(1)}(t)$. Time scale t_0 is $Y_0/\sqrt{gH_00}$ and T is duration of sampling

bay the maximum runup found from Dirichlet condition $\eta|_{x=x_0^-} = 2\eta^{\text{open}}_{\text{inc}}\Big|_{x=x_0^+}$ is 4 when the perturbation $r^{(1)}$ is added the maximum runup is reduced to 3.6, the 'exact' runup from the integral equation is 3.52 .

V. CONCLUSION

We have shown that the problem a wave packet entering a narrow non-reflecting bay can be reduced to one dimensional problem. The resulting one dimensional problem admits

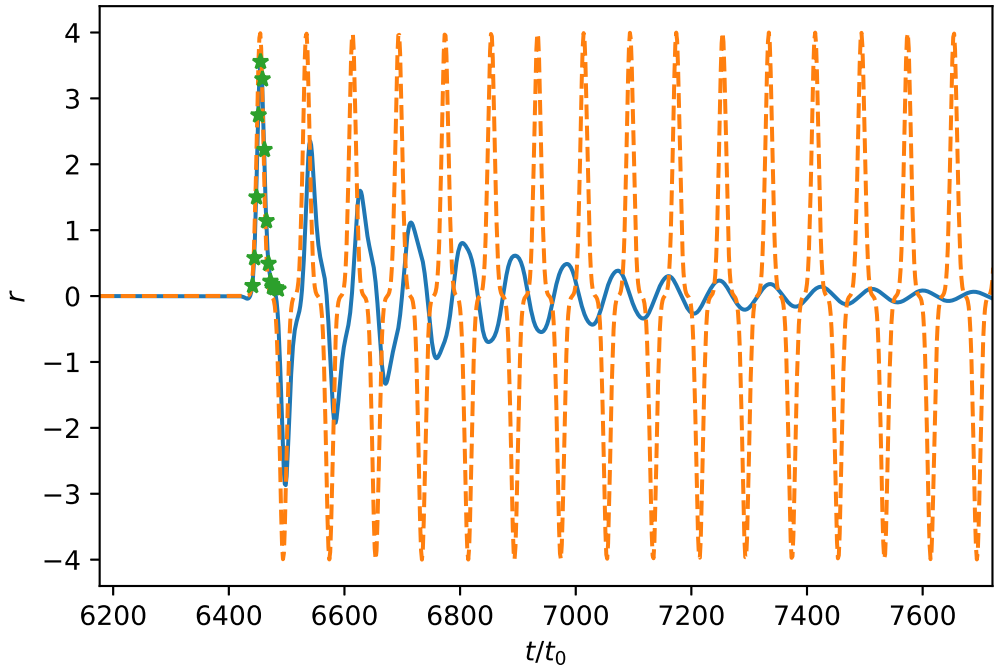

FIG. 9. Runup generated by a gaussian incident wave given by $\exp\left(-\left((x+\sqrt{gH_0}(t-T/2)/(0.4x_0)\right)^2\right)$ entering a rectangular bay of aspect ratio $x_0/(2Y_0)=10$. Continuous curve is the solution of integral equation, broken curve is $r^{(0)}(t)$ (undisturbed solution of Dirichlet problem), the stars are $r^{(0)}(t)+r^{(1)}(t)$. Time scale t_0 is $Y_0/\sqrt{gH_00}$ and T is duration of sampling. Maximum runup associated with $r^{(0)}$ and $r^{(0)}+r^{(1)}$ are 4.0 and 3.6 respectively. The 'exact' maximum runup associated with the integral equation is 3.52 .

solution in closed form if asymptotic approximation of function $\Gamma(\tau)$ are made for large and small τ.

Appendix A: Generalised eigenvalue problem

In this appendix how the regular solution of ordinary equation given by (20) can be found using linear algebra package for Python computer language. The emphasis will be on the easy implementation rather than the speed of computation. First insert the series in (22) into (20). When one multiplies the resulting series by $\sqrt{2n+0.5}P_{2n}(y')$ and integrate the product from -1 to 1 a linear relation between A^{κ}_{2l}'s is found. The procedure will be

repeated M times with $\sqrt{0.5}P_0(y'), \sqrt{2+0.5}P_2(y'), .., \sqrt{(2M-2)+0.5}P_{2M-2}(y')$, to get M relations between coefficients A^{κ}_{2l} . These relations can be written as

$$-(k^{\rm inc}_{\rm open}Y_0)^2\left(\sum_{q=0}^{2M-1}\delta_{nq}A^{\kappa}_{(2q)}\right)-\kappa^2Y_0^2\left(\sum_{q=0}^{2M-1}T_{nq}A^{\kappa}_{(2q)}\right)$$
$$+\sum_{q=0}^{2M-1}\delta_{nq}2q(2q+1)A^{\kappa}_{(2q)}=0\quad\text{for}\quad n=0,1,..,M-1\,. \tag{A1}$$

Here $\delta_{nq}=\int_{-1}^{1}dy'\sqrt{2n+0.5}P_{2n}(y')\sqrt{2q+0.5}P_{2q}(y')$ is Knocker delta with $\delta_{nq}=1$ for $n=q$ and zero for $n\neq q$. Integral T_{nq} is given by

$$T_{nq}=\int_{-1}^{1}dy'\sqrt{2n+0.5}P_{2n}(y')(1-y'^2)\sqrt{2q+0.5}P_{2q}(y')\,. \tag{A2}$$

It is clear from the expression above matrix $\mathbf{T}$ is a symmetrical tridiagonal matrix ($T_{ij}=0$ for $|i-j|>1$) because Legendre polynomial of degree $2n$ is orthogonal to *all* polynomials of degree less than $2n$ and in (A2) expression $(1-y'^2)P_{2q}(y')$ is a polynomial of degree $2(q+1)$.

Although the integrals in (A2) can be analytically calculated using recurrence relation of Legendre polynomials it is more practical to proceed to numerical integration because these integrals should be executed only once for all frequencies.

Equation (A1) can be cast in matrix form as

$$(\kappa Y_0)^2\mathbf{T}\left(A_0,A_2,..,A_{2M-2}\right)^T=\mathbf{D}\left(A_0,A_2,..,A_{2M-2}\right)^T\,. \tag{A3}$$

where superscript T denotes transpose and $\mathbf{D}$ is diagonal matrix with $D_{n,n}=2n(2n+1/2)-(k^{\rm inc}_{\rm open}Y_0)^2$. The equation above is called generalised eigenvalue problem because eigenvalue $(\kappa Y_0)^2$ is multiplied by matrix $\mathbf{T}$ rather then identity matrix. Here $\mathbf{T}$ is a positive definite matrix because $\int_{-1}^{1}dy'(1-y'^2)f^2(y')>0$. The usual method to transform a generalised eigenvalue problem to an ordinary eigenvalue problem without loosing the symmetrical nature of matrices is to proceed Cholesky decomposition of the positive matrix,

$$\mathbf{T}=\mathbf{S}\mathbf{S}^T$$

where $\mathbf{S}$ is a lower triangular matrix. Defining new variables

$$\left(A^*_0,A^*_2,..,A^*_{2M-2}\right)^T=\mathbf{S}^T(A_0,A_2,..,A_{2M-2})^T \tag{A4}$$

and rewriting A3 in terms of the new variables leads to

$$(\kappa Y_0)^2\mathbf{T}\mathbf{S}^{-1^T}\left(A^*_0,A^*_2,..,A^*_{2M-2}\right)^T=\mathbf{D}\mathbf{S}^{-1^T}\left(A^*_0,A^*_2,..,A^*_{2M-2}\right)^T$$

When equation above is multiplied from left by $\mathbf{S}^{-1}$ on has an eigenvalue problem associated with a symmetrical matrix

$$(\kappa Y_0)^2 \left(A_0^*, A_2^*, .., A_{2M-2}^*\right)^T = \mathbf{S}^{-1}\mathbf{D}\mathbf{S}^{-1^T}(A_0^*, A_2^*, .., A_{2M-2}^*)^T . \tag{A5}$$

The eigenvectors of the generalised eigenvalue problem can be restored multiplying eigenvectors of $\mathbf{S}^{-1}\mathbf{D}\mathbf{S}^{-1^T}$ by matrix $\mathbf{S}^{-1^T}$. All these steps are carried out with a single call of function `linalg.eigh(D,T)` from `numpy` package for Python. All the eigenvectors of the generalised eigenvalue problem are found by routine `eigh`. Only the ones that conform to convergence criteria will be retained ($A_{2l} \to 0$ for $2l$ approaching M). Routine `eigh` returns eigenvalues in ascending order. In general the first half of the eigenvectors meet the convergence criteria.

To transform a generalised eigenvalue problem in (A3) It would have been easier to multiply $\mathbf{T}$ from right and left by the diagonal matrix, $\mathbf{D}^{-1/2}$. The matrix resulting from this multiplication will be tridiagonal. We did not resort to this method because for some frequencies matrix $\mathbf{D}$ can be singular.

Appendix B: Variational formulation eigenvalues associated the decaying modes

For a given frequency ω ,eigenvalues $(\kappa Y_0)^2$ associated decaying modes are the local minimum of the Rayleigh quotient

$$\min_{\mathbf{A}} \frac{\mathbf{A}\mathbf{D}(\omega)\mathbf{A}^T}{\mathbf{A}\mathbf{T}\mathbf{A}^T} \tag{B1}$$

where $\mathbf{A}$ is the row vector $(A_0, A_2, .., A_{2M-2})$. The absolute minimum of the Rayleigh quotient is related to the wave vector of the energy transmitting mode.

---

[1] C. E. Synolakis, The runup of solitary waves, Journal of Fluid Mechanics **185**, 523–545 (1987).

[2] G. F. CARRIER, T. T. WU, and H. YEH, Tsunami run-up and draw-down on a plane beach, Journal of Fluid Mechanics **475**, 79–99 (2003).

[3] M. ANTUONO and M. BROCCHINI, Solving the nonlinear shallow-water equations in physical space, Journal of Fluid Mechanics **643**, 207–232 (2010).

[4] T. S. Stefanakis, F. Dias, and D. Dutykh, Local run-up amplification by resonant wave interactions., Physical review letters **107 12**, 124502 (2011).

[5] S. Stefanakis, T., S. Xu, D. Dutykh, and F. Dias, Run-up amplification of transient long waves, Q. Appl. Math. **73** (2015).

[6] A. Ezersky, D. Tiguercha, and E. Pelinovsky, Resonance phenomena at the long wave run-up on the coast, Natural Hazards and Earth System Sciences **13**, 2745 (2013).

[7] N. Postacioglu, M. S. Özeren, and U. Canlı, On the resonance hypothesis of storm surge and surf beat run-up, Natural Hazards and Earth System Sciences **17**, 905 (2017).

[8] I. Didenkulova and E. Pelinovsky, Runup of tsunami waves in u-shaped bays, PURE APPL GEOPHYS. **168**, 1239 (2011).

[9] G. Pedersen, Fully nonlinear boussinesq equations for long wave propagation and run-up in sloping channels with parabolic cross sections, Natural Hazards **84**, 599 (2016).

[10] T. Shimozono, Long wave propagation and run-up in converging bays, Journal of Fluid Mechanics **798**, 457–484 (2016).

[11] C. Mei, c, *The Applied Dynamics of Ocean Surface Waves* (World Scientific, 1992).

[12] E. Pelinovsky and R. KH.Mazova, Exact analytical solutions of nonlinear problems of tsunami wave run-up on slopes with different profiles, Nat. Hazards **6**, 227 (1992).

[13] E. Pelinovsky and R. K. Mazova, Exact analytical solutions of nonlinear problems of tsunami wave run-up on slopes with different profiles, Natural Hazards **6**, 227 (1992).

[14] A. Baran and U. Kânoḡlu, Wind set-down relaxation, CMS **21**, 149 (2007).

[15] U. KÂNOḠLU and C. E. SYNOLAKIS, Long wave runup on piecewise linear topographies, Journal of Fluid Mechanics **374**, 1–28 (1998).

[16] M. Abromowitz and A. Stegun, I., *Handbook of mathematical functions* (Dover, 1972).

[17] B. Whitham, G., *Linear and nonlinear waves* (John Wiley and Sons, 1973).

[18] D. Nicolsky, E. Pelinovsky, A. Raz, and A. Rybkin, General initial value problem for the nonlinear shallow water equations: Runup of long waves on sloping beaches and bays, Physics Letters A **382**, 2738 (2018).

[19] I. Didenkulova and E. Pelinovsky, Nonlinear wave evolution and runup in an inclined channel of a parabolic cross-section, Phys. Fluids **23**, 086602 (2011).